Advances in Water Resources 62 (2013) 90–105

Contents lists available at ScienceDirect

Advances in Water Resources

journal homepage: www.elsevier.com/locate/advwatres

Optimization of stomatal conductance for maximum carbon gain under dynamic soil moisture

Stefano Manzoni [a,b,*], Giulia Vico [a], Sari Palmroth [c,d], Amilcare Porporato [b,c], Gabriel Katul [b,c]

[a] Department of Crop Production Ecology, Swedish University of Agricultural Sciences, SE-750 07 Uppsala, Sweden
[b] Department of Civil and Environmental Engineering, Duke University, Box 90287, Durham, NC 27708-0287, USA
[c] Nicholas School of the Environment, Duke University, Box 90328, Durham, NC 27708, USA
[d] Department of Forest Ecology and Management, Swedish University of Agricultural Sciences, SE-901 83 Umeå, Sweden

ARTICLE INFO

Article history:
Received 28 May 2013
Received in revised form 23 September 2013
Accepted 26 September 2013
Available online 9 October 2013

Keywords:
Optimization
Photosynthesis
Soil moisture
Stomatal conductance
Transpiration

ABSTRACT

Optimization theories explain a variety of forms and functions in plants. At the leaf scale, it is often hypothesized that carbon gain is maximized, thus providing a quantifiable objective for a mathematical definition of optimality conditions. Eco-physiological trade-offs and limited resource availability introduce natural bounds to this optimization process. In particular, carbon uptake from the atmosphere is inherently linked to water losses from the soil as water is taken up by roots and evaporated. Hence, water availability in soils constrains the amount of carbon that can be taken up and assimilated into new biomass. The problem of maximizing photosynthesis at a given water availability by modifying stomatal conductance, the plant-controlled variable to be optimized, has been traditionally formulated for short time intervals over which soil moisture changes can be neglected. This simplification led to a mathematically open solution, where the undefined Lagrange multiplier of the optimization (equivalent to the marginal water use efficiency, λ) is then heuristically determined via data fitting. Here, a set of models based on different assumptions that account for soil moisture dynamics over an individual dry-down are proposed so as to provide closed analytical expressions for the carbon gain maximization problem. These novel solutions link the observed variability in λ over time, across soil moisture changes, and at different atmospheric CO_2 concentrations to water use strategies ranging from intensive, in which all soil water is consumed by the end of the dry-down period, to more conservative, in which water stress is avoided by reducing transpiration.

© 2013 Elsevier Ltd. All rights reserved.

1. Introduction

The dynamics of biological systems, from cells to communities and ecosystems, have been hypothesized to follow optimal trajectories shaped by selection pressure that force organisms to maximize their fitness and reproductive success [1]. This concept has been particularly successful in explaining the form and function of terrestrial vegetation from ecohydrological and carbon-economy perspectives, and across spatial and temporal scales [2–15]. Any optimality model is based on three key ingredients: an objective function that describes the gain that needs to be maximized or loss to be minimized, a control variable that shifts the dynamics in the desired direction, and a set of constraints that account for environmental conditions and conservation laws bounding the system [16]. All three ingredients are difficult to define and quantify – especially in complex biological and ecological systems. Despite these difficulties, optimality approaches may complement process-based approaches when mechanistic knowledge is scarce.

With regards to the definition of a proper objective function, thermodynamic considerations suggest that thermodynamic fluxes and entropy production should be extremized [8,17–21]. As a consequence of this maximization principle, hydrological fluxes through the soil–plant–atmosphere continuum should also be maximized [22–24]. From an ecological perspective, it has been argued that plants maximize their growth rate [25], which is linked to reproductive capacity [26]. Accordingly, a number of theories are based on the assumption that the plants aim at maximum carbon (C) uptake and growth (subject to constraints) over a given period [8,13,14,27–29]. Within the context of coupled hydrologic-biogeochemical models, the maximization of net carbon gain can be achieved by maximizing carbon uptake by leaves [4,30,31] – a key premise to the results presented here.

To be effective, the control variable of the optimization problem should be able to impose the optimal 'decisions' over key elements of plant functioning. Hence, the choice of the control variable depends on the time scale of interest and the most important tradeoffs the plant faces at that particular scale. Here, the focus is on time scales commensurate with the inter-storm period that

* Corresponding author at: Department of Crop Production Ecology, Swedish University of Agricultural Sciences, SE-750 07 Uppsala, Sweden. Tel.: +46 (0)18 671418.
E-mail address: stefano.manzoni@slu.se (S. Manzoni).

0309-1708/$ - see front matter © 2013 Elsevier Ltd. All rights reserved.
http://dx.doi.org/10.1016/j.advwatres.2013.09.020

varies between days or several weeks, depending on the climatic regime. Also, the deterministic dynamics of an individual dry-down are first considered, as a first step towards a more general stochastic framework to be developed in a separate contribution in which the inter-storm period and rainfall amounts are random. Stomatal movements occur at much shorter time scales, allowing a fine-scale regulation of CO_2 and water vapor exchanges [32,33]. Therefore, stomatal conductance can be considered an effective control variable [31,34], as also pointed out in a seminal paper by van den Honert, "It is clear that the regulators of the water transport, the stomata, are inserted in the gaseous part, where they control the master-process by varying the diffusion resistance. Regulators could be nowhere else." [35, p. 152]. Despite other regulators are employed at these time scales, including aquaporins [36] and leaf xylem tissues, which are allowed to partially cavitate, thus acting as an 'hydraulic fuse' [37,38], stomata remain among of the main water loss control points. Changes in leaf nitrogen concentration affecting the biochemical machinery [13,39], stomatal size and density [40,41], and plant allocation patterns [11,42] can also be used to regulate C gains and water losses, but at time scales that are much longer than an individual dry-down considered here.

Stomatal regulation is constrained by the basic condition that the amount of water available in the root zone is finite and that such water store decreases at a rate that is directly proportional to stomatal aperture [43,44]. Therefore, opening stomata to allow carbon uptake intrinsically causes water depletion, increasing the likelihood of water stress (either in form of reduced hydraulic functionality, or as metabolic limitations to photosynthesis) and thus shortening the duration of the photosynthetically-active period. This tradeoff between carbon uptake and water consumption, its mathematical formulation, and consequences on plant functioning and the soil water balance, frames the scope of this contribution.

The addition of a constraint in the optimization problem can be mathematically achieved by introducing a Lagrange multiplier (or co-state variable), here denoted by λ (see Section 2), which directly affects the control variable. This additional variable is in general time-dependent and can be computed if the conditions at the boundaries of the problem are known [16]. In the case of stomatal control, such boundaries are defined by the initial and final water availability during the period considered [43]. In most previous studies on stomatal optimization, the function $\lambda(t)$ has been treated as an unknown, often constant multiplier estimated as a fitting parameter [40,45–48]. Models accounting for variations in λ generally assume that it may change as a function of water availability through empirical formulations that are de-coupled from the optimization problem [49–53], even though the function $\lambda(t)$ should be part of the optimization procedure (as illustrated by the time trajectories in Fig. 1). Here, changes in λ through time and as a function of environmental conditions are explicitly included by means of a sequence of minimal plant models. Understanding the theoretical underpinning of changes in λ and stomatal conductance might provide models of canopy and ecosystem gas exchanges with compact formulations that capture plant effects on these exchanges.

The paper is organized as follows: the optimization problem is first formulated in the most general terms highlighting the role of a dynamic λ, the constraints, and the boundary conditions (Section 2). Next, a sequence of optimization models is developed by exploring the role of different terms in the objective function and formulation of water availability constraints (Section 3). For each model, the optimal solutions are compared with previous theoretical and empirical results.

2. Theory

The general theory of optimal control of plant gas exchange under variable soil water conditions is presented in Section 2.1 and the constitutive equations for the water fluxes are discussed in Sections 2.2–2.4. All symbols are listed and defined in Table 1. It is also important to emphasize that in this derivation, plants are assumed to control g directly, while in reality the stomatal aperture is being regulated (Appendix A shows that the optimality solutions are not affected by this assumption).

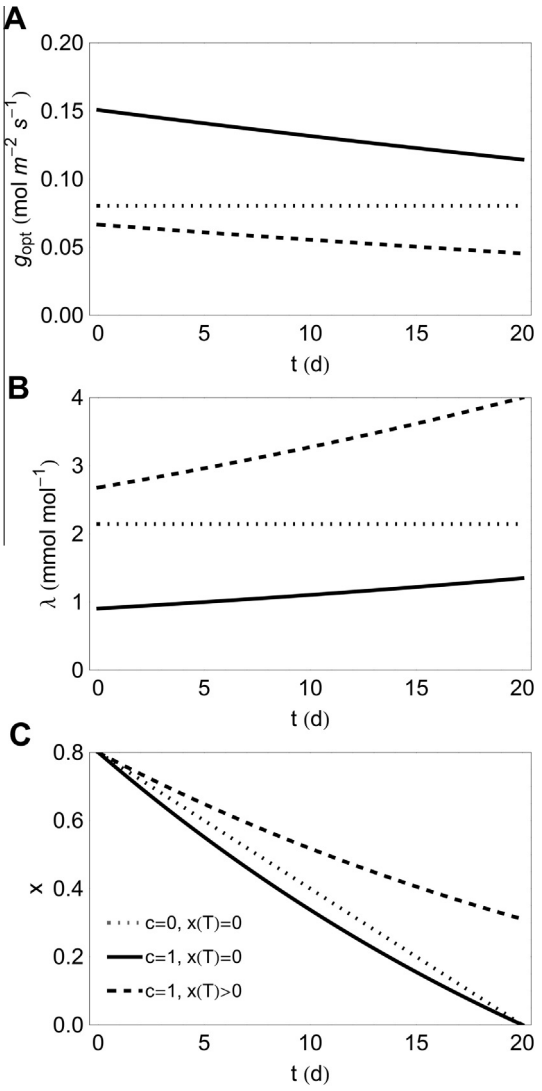

Fig. 1. Time trajectories of (A) stomatal conductance (g_{opt}), (B) Lagrange multiplier (λ), and C) plant-available soil moisture (x) when stomatal conductance is optimized to achieve maximum carbon gain (plus a terminal gain) over a dry-down of known duration, T. Line styles denote different optimization approaches: constant and linear uncontrolled losses ($c = 0$ and $c = 1$ in Eq. (15)) for a set terminal state, $x(T) = 0$ (dotted and solid curves, respectively), and linear uncontrolled losses with free terminal state (dashed curves). In all panels, $T = 20$ days, $D = 0.015$ mol mol^{-1}, $c_a = 350$ μmol mol^{-1}, $k = 0.05$ mol m^{-2} s^{-1}, $r = 0$, $\gamma = 10$ mm d^{-1}, $Z_r = 0.3$ m, $n = 0.5$, and $\Lambda = 170 \times T_{day}$ μmol m^{-2}.

2.1. A general formulation for the optimization of carbon uptake by plants

The following optimization assumes that plants maximize their C uptake (A) over a period T, plus an additional C gain at the end of such period that depends on the final soil moisture status and accounts for long-term water stress damage. This assumption can be formalized by the objective function J,

$$J = \int_0^T A[g(t), x(t), t]dt + J_T, \tag{1}$$

Table 1
Definition of symbols used in the main text (other parameters are defined in the Appendices). Subscripts '0' and '*b*' respectively refer to initial conditions and soil moisture-limited variables; superscript '$*$' indicates the transition point between free stomatal control and soil moisture-limited regime.

Symbol	Definition	Units
a	Ratio of water vapor to CO_2 diffusivity, $a = 1.6$	–
A	Photosynthetic rate	$\mu mol\ m^{-2}\ s^{-1}$
α	Combination of parameters, $\alpha = va(nZ_r)^{-1}$	$m^2\ s\ mol^{-1}\ d^{-1}$
β	Combination of parameters, $\beta = \gamma(nZ_r)^{-1}$	d^{-1}
c	Exponent of the water loss function	–
c_i	Internal CO_2 concentration	$\mu mol\ mol^{-1}$
c_a	Atmospheric CO_2 concentration	$\mu mol\ mol^{-1}$
C	Inequality constraint, $C(g,x) = g - g_b(x) \leqslant 0$	$mol\ m^{-2}\ s^{-1}$
γ	Parameter of the water loss function	$m\ d^{-1}$
D	Vapor pressure deficit	$mol\ mol^{-1}$
E	Transpiration rate	$m\ d^{-1}$
E_{SR}	Soil-moisture limited water supply to the roots	$m\ d^{-1}$
f	Right hand side of the soil moisture balance equation, $f = -(E+L)/(nZ_r)$	d^{-1}
g	Stomatal conductance to CO_2	$mol\ m^{-2}\ s^{-1}$
g_a	Atmospheric conductance to CO_2	$mol\ m^{-2}\ s^{-1}$
g_b	Soil moisture-limited stomatal conductance, $g_b = \kappa\ x_b/(\alpha D)$	$mol\ m^{-2}\ s^{-1}$
g_{opt}	Optimal stomatal conductance to CO_2	$mol\ m^{-2}\ s^{-1}$
H	Hamiltonian of the optimization, $H = A + \lambda f$	$\mu mol\ m^{-2}\ s^{-1}$
H	Augmented Hamiltonian for the soil moisture-limited regime, $\mathrm{H} = H + \mu\ C$	$\mu mol\ m^{-2}\ s^{-1}$
J	Objective function (net carbon gain)	$\mu mol\ m^{-2}$
J_T	Terminal carbon gain, $J_T = \Lambda x$	$\mu mol\ m^{-2}$
k	Carboxylation efficiency	$mol\ m^{-2}\ s^{-1}$
κ	Combination of parameters, $\kappa = k_{SR}(nZ_r)^{-1}$	d^{-1}
k_{SR}	Proportionality constant for the soil-root water supply rate	$m\ d^{-1}$
L	Water losses not controlled by plants (runoff and leakage below the rooting zone)	$m\ d^{-1}$
LAI	Leaf area index	$m^2\ m^{-2}$
λ, λ_0, λ^*	Lagrange multiplier of the optimization	$\mu mol\ d\ m^{-2}\ s^{-1}$ or $mmol\ mol^{-1}$
Λ	Proportionality constant for the terminal C gain	$\mu mol\ m^{-2}$
M_w	Molar mass of water, $M_w = 0.018$	$kg\ mol^{-1}$
μ	Lagrange multiplier for the soil moisture-limited regime	–
n	Soil porosity	$m^3\ m^{-3}$
v	Unit conversion factor, $v = \mathrm{LAI}T_{day}M_w/\rho_w$	$m^3\ s\ mol^{-1}\ d^{-1}$
t, t^*	Time	d
T	Time interval	d
T_{day}	Day length in seconds	$s\ d^{-1}$
r	Respiration rate	$\mu mol\ m^{-2}\ s^{-1}$
R	Rainfall input	$m\ d^{-1}$
ρ_w	Density of liquid water, $\rho_w = 10^3$	$kg\ m^{-3}$
x, x_0, x^*	Plant-available relative volumetric soil moisture	–
χ	Fraction of initial soil moisture	–
Z_R	Rooting depth	m

where J_T represents the C gain at the end of the time period T (thereafter referred to as terminal gain). The net C uptake, A, is expressed as a function of stomatal conductance to CO_2, $g(t)$, plant-available soil moisture averaged over the rooting depth, $x(t)$, and time ($t \in [0, T]$). For notational simplicity, the relative soil moisture is normalized by the fraction of plant-available soil water (i.e., between the wilting point and saturation), so that the variable $x(t)$ varies between 0 and 1. Separating the effects of these three sources of variation in photosynthesis allows disentangling purely diffusive limitations due to $g(t)$ [32], metabolic limitations at low $x(t)$ [54], and time-varying environmental conditions (e.g., photosynthetically-active radiation and vapor pressure deficit fluctuations).

At the end of the dry-down period, plants experience the most stressing conditions, which may involve physiological C costs to repair damaged tissues and restore functionality. The terminal gain J_T accounts for these long-term consequences of water stress events. The rationale behind this contribution is that plants have to spend resources to repair the damages caused by a prolonged water stress period (e.g., refilling of embolized tissues; re-growth of damaged leaves and branches). Such costs can be avoided by closing stomata, so that at the end of the dry-down period enough water remains available to prevent damage. Hence, J_T represents the amount of C that can be 'saved' by avoiding low soil moisture values and hence limiting these costs. As discussed in the following, the value of J_T affects the shape of the optimal trajectories, as J_T shifts the relative importance of C uptake *vs.* water conservation. Thus, J_T encodes the long-term water-use strategy of the plant, with lower values of J_T indicating more intense soil water depletion associated with aggressive water use strategies. Conversely, higher values of J_T are associated with conservative water use strategies.

The amount of water available for plant uptake and transpiration is constrained by the water balance in the rooting zone, which represents the 'dynamic resource constraint' of this optimization problem. For analytical tractability, a lumped approach is employed where the vertically-averaged plant-available soil moisture is considered and the fluxes are interpreted as whole canopy exchanges with the atmosphere. The mass balance equation for soil moisture can be expressed as [5,43]

$$nZ_r \frac{dx}{dt} = R(t) - E[g(t), t] - L[x(t), t], \tag{2}$$

where $R(t)$ is the rainfall input, n is the soil porosity, Z_r is the mean rooting depth, E is the transpiration from the plant canopy, and L includes leakage and other water losses that cannot be directly controlled by plants. The initial value of soil moisture is assumed to be known and is denoted by $x(0) = x_0$. The focus here is on a period without rain ($R = 0$) during which the water loss function $f = -(E + L)/(nZ_r)$ is defined, and Eq. (2) can be expressed as $dx(t)/dt = f[g(t), x(t), t]$.

2.1.1. Free stomatal control of transpiration

Based on Eqs. (1) and (2), the goal is to derive the time trajectory of $g(t)$ that maximizes J. To solve this optimal control problem, the so-called Hamiltonian is constructed, along with the necessary conditions for optimality [16,55]. These conditions rest on the assumption that all the functions involved are differentiable. Discontinuities such as transitions between free stomatal control and soil moisture-limited transpiration need to be treated as added constraints (Section 2.1.2). When the stomatal conductance is not bound by soil moisture limitations, the Hamiltonian is given by the sum of the integrand of Eq. (1) and the right hand side of Eq. (2), multiplied by the Lagrange multiplier $\lambda(t)$,

$$H[g(t),x(t),t] = A[g(t),x(t),t] + \lambda(t) f[g(t),x(t),t], \tag{3}$$

where $\lambda(t)$ is only a function of time and due to the different units of A and f, it is expressed in μmol d m^{-2} s^{-1}. To convert λ to conventional units of mmol mol^{-1}, a multiplying factor $v/(10^3 nZ_r)$ is needed, where $v = \mathrm{LAI} T_{day} M_w/\rho_w$ (see Table 1 for symbol definitions). Also, note that λ is defined as the inverse of the multiplier (with the same symbol) adopted by Cowan and Farquhar [30]. The necessary conditions for optimum $g(t)$ are found as (dropping the functional dependencies for notational simplicity)

$$\frac{\partial H}{\partial g} = \frac{\partial A}{\partial g} + \lambda \frac{\partial f}{\partial g} = 0, \tag{4}$$

$$\frac{d\lambda}{dt} = -\frac{\partial H}{\partial x}. \tag{5}$$

For given functional relations between photosynthesis and stomatal conductance (Section 2.2), and between the water loss function and stomatal conductance (Section 2.3), Eq. (4) becomes an algebraic equation that provides a link between the control variable and the Lagrange multiplier. Eq. (5) is instead the differential equation regulating the temporal changes of λ, with an initial condition λ_0 that depends on the specific formulation chosen (as discussed in Section 3.1) [16]. Furthermore, Eq. (4) allows us to interpret the Lagrange multiplier as the marginal water use efficiency, $\lambda = \partial A/\partial g(\partial E/\partial g)^{-1}$, when the only effect of stomatal conductance on the loss function f is through transpiration. Eqs. (2), (4) and (5) represent a system of algebraic-differential equations that fully define the optimal trajectory of stomatal conductance. Again, the function $\lambda(t)$ is determined by Eq. (5), and should not be considered as an 'external' parameter, but rather a result of the optimization (Fig. 1).

2.1.2. Soil moisture-limited transpiration

If stomatal conductance is not entirely free, but it is limited by water supply from the bulk soil to the roots, the optimal trajectories need to account for this additional constraint. We denote this 'soil moisture-limited' stomatal conductance by $g_b(x)$, where the subscript 'b' indicates that the control variable lies on a boundary of its domain, as opposed to be completely free (subscript '*opt*'). The resulting mixed inequality constraint (involving both control and state variable) can be formulated as $g \leqslant g_b(x)$, or $C(g,x) = g - g_b(x) \leqslant 0$. To proceed in the solution, an 'augmented Hamiltonian' is introduced (details on this approach are presented in, e.g., [55]),

$$\mathrm{H}[g(t),x(t),t] = H[g(t),x(t),t] + \mu[x(t),\lambda(t)] C[g(t),x(t)], \tag{6}$$

where H is defined by Eq. (3) and μ is an additional Lagrange multiplier, which can be computed by imposing the condition $\partial \mathrm{H}/\partial g = 0$ (for convenience, we drop the time dependencies),

$$\mu(x,\lambda) = -\frac{\partial \mathrm{H}}{\partial g}\left(\frac{\partial C}{\partial g}\right)^{-1}\Bigg|_{g=g_b(x)} \tag{7}$$

if stomatal conductance is constrained, and $\mu = 0$ otherwise. When the stomatal conductance is limited by soil moisture, the Lagrange multiplier λ departs from the trajectory described by Eq. (5) and can be obtained from,

$$\frac{d\lambda}{dt} = -\frac{\partial \mathrm{H}}{\partial x}. \tag{8}$$

Notably, under this soil moisture-limited regime, λ does not satisfy Eq. (4) in the whole temporal domain and therefore cannot be interpreted as marginal water use efficiency, as in the unconstrained case.

2.2. Stomatal control of transpiration and photosynthesis

The solution of both the unconstrained and the soil moisture-limited problems depends on how photosynthesis (A), transpiration (E), the water loss term (L), and the final gain (J_T) are specified. Both transpiration and photosynthesis depend on the control variable g, interpreted as a canopy-averaged stomatal conductance. The water vapor flux between the stomatal cavity (assumed saturated at the leaf temperature) and the atmosphere can be described through a series of conductances (stomatal, g, and aerodynamic, g_a) linking water vapor concentration in the stomatal cavity and in the atmosphere via,

$$E = v\frac{a g g_a}{g + g_a} D \approx v a g D, \tag{9}$$

where D is the difference between the concentrations of water vapor at saturation (in the stomatal cavity) and in the bulk atmosphere, $a = 1.6$ is the ratio of the diffusivities of water vapor and CO_2, and v converts units typically used for stomatal conductance (mol m^{-2} leaf s^{-1}) to units consistent with the water balance in Eq. (2) (i.e., m^3 m^{-2} ground d^{-1}). For simplicity, it is assumed that the canopy is well-coupled with the atmosphere (e.g., as in the case of sparse canopies, for species with small leaves, or for high mean wind conditions), so that $g \ll g_a$ and $E \approx vagD$.

The function $A[g(t),x(t),t]$ in Eq. (1) embeds the effects of both $g(t)$ and the moisture availability, $x(t)$, on the objective function. Hence, the specific shape and nonlinearity of $A[g(t),x(t),t]$ affects the optimal solution. A derivation of this relation is reported in Appendix B and only the main result is presented. We assume that photosynthesis is proportional to the CO_2 concentration inside the stomatal cavity, c_i [56–58] and that CO_2 transport across the stomata is driven by diffusion, in analogy to Eq. (9). Combining the equations representing CO_2 diffusion and photosynthetic rate (Eqs. (34) and (35)), neglecting respiration, and eliminating c_i yields the relation between A and g that is needed to formulate the optimization problem [47,56,59],

$$A = \frac{g c_a k}{g + k}, \tag{10}$$

where k is the carboxylation efficiency (assumed independent of x) and c_a is the atmospheric CO_2 concentration. Thus, with these assumptions, direct soil moisture effects on A (e.g., metabolic limitations) are neglected.

2.3. Deep percolation and transpiration by competing plants

Leakage losses, soil water evaporation, and transpiration by competing plants depend on soil moisture in complex ways, which could be partly captured by expressing the water loss function L in the balance Eq. (2) as a nonlinear function of soil moisture [5]. The simplest approach is to assume that these 'uncontrolled' losses vary as

$$L[x(t)] = \gamma\, x(t)^c, \tag{11}$$

where the parameter c describes the degree of dependence of such losses on soil moisture. For analytical tractability, the analyses are

confined to the cases of $c = 0$, representing uncontrolled water losses that are independent of soil moisture, or $c = 1$ when such losses are simply proportional to soil moisture. These values of the exponent c are chosen to allow analytical tractability, but the nonlinear increase in water losses with increasing x when the soil is close to saturation is neglected [5]. Nevertheless, below the soil field capacity (as in the case studies considered here) and without more detailed information, this linearized formulation may approximate water losses due to compound evaporation and transpiration by competing plants [60]. Conversely, the value of the empirical parameter γ can be estimated as the saturated hydraulic conductivity if the uncontrolled losses are mainly due to drainage below the rooting zone, or as a fraction of the potential evapotranspiration if uncontrolled losses are due to combined evaporation and transpiration by other competing plants. The parameter γ is equal to zero if transpiration is the only water loss term in the soil moisture balance (e.g., no competing plants and negligible deep percolation).

2.4. Soil moisture limitations to transpiration

Eq. (9) describes transpiration as fully controlled by stomatal conductance. However, as soil moisture decreases, water transport in the soil-root system slows down due to decreasing soil hydraulic conductivity. Hence, in dry conditions, soil moisture may limit water supply to the roots, thus constraining transpiration and hence the variation of the optimal g. This effect is accounted for by setting an upper bound to transpiration that depends on soil moisture (E_{SR}), but not on stomatal conductance. This supply-limited flux is proportional to the soil hydraulic conductivity and also depends on rooting depth and root area density [61].

To investigate this limitation to transpiration while retaining analytical tractability, we employ the linear relation,

$$E_{SR}[x(t)] = k_{SR}\, x(t), \tag{12}$$

where k_{SR} is a proportionality constant (with units of m d^{-1}). Eq. (12) neglects two nonlinearities, namely the nonlinear dependences of hydraulic conductivity (buffered by fine root growth, see [62]) and soil water potential on soil moisture, but it still approximates the soil moisture limitation mechanism by including the effect of water availability on soil-to-root water transport. By linearizing the hydraulic conductivity, Eq. (12) might overestimate E_{SR} at low x and underestimate it wet conditions, in which, however, stomatal control is more likely. In contrast, neglecting the effect of soil water potential on the driving force of E_{SR} (i.e., the water potential difference between bulk soil and roots) is likely less important, because pressure drops between components of the soil–plant system tend to be stable.

Comparing Eqs. (9) and (12), the upper bound for stomatal conductance, $g_b(x)$, is obtained,

$$g \leqslant g_b(x) = \frac{k_{SR}}{vaD} x_b(t). \tag{13}$$

2.5. Model parameterization and testing

To test the model, two studies where atmospheric CO_2 concentration in the growth environment was manipulated are considered: the Duke Forest Free Air CO_2 Enrichment site (FACE, located in Durham, NC, USA) and the Lysimeter CO_2 Gradient facility (LYCOG, located in Temple, TX, USA). A detailed description of experimental setup and environmental conditions can be found elsewhere [63–65]. We also selected a study reporting gas exchange measurements during an extended dry-down period to assess the effect of soil moisture limitations on the optimal solutions [66]. Here, the details of model parameter estimation are provided and Table 3 reports all the relevant parameter values.

Gas exchange data for *Pinus taeda*, the dominant tree species at the Duke Forest FACE site, and the C_3 herb *Solidago canadensis* and the C4 grass *Sorghastrum nutans* from the LYCOG facility were considered. Carboxylation rates were obtained from published $A(c_i)$ curves [50,64] and assumed constant with respect to c_a (Table 3). Specifically, for the two herbaceous species, nonlinear $A(c_i)$ curves (Eq. (36)) were fitted to the light-saturated gas exchange data to obtain temperature-corrected parameters a_1 and a_2. Finally, the carboxylation rate was estimated as $k \approx a_1/(a_2 + rc_a)$, where r indicates the long-term c_i over c_a ratio, and c_a was taken to be ambient atmospheric CO_2 concentration (letting c_a change in the expression for k does not significantly alter the results). Temperature corrections were calculated following Campbell and Norman [67]. The typical daytime vapor pressure deficits at Duke Forest is $D = 0.015$ mol mol^{-1}, while at the LYCOG facility VPD during the measurement period was around $D = 0.03$ mol mol^{-1}. We selected this relatively high VPD value assuming it was representative of mid-summer growth conditions, even though on average VPD is lower [63]. The leaf area index (LAI) is around 1.5 and 4 for the herbaceous species and for *P. taeda*, respectively. Parameter β is estimated by assuming that uncontrolled losses due to competition with other plants, soil evaporation, and deep percolation are about half the potential evapotranspiration for the grasses, which were growing in competition with other species. In contrast, we assume that uncontrolled losses are ¼ of the potential evapotranspiration in the *P. taeda* monoculture, where only limited competition by understory species occurs. The time scale for a complete drying from well-watered conditions was estimated as five times the mean rainfall inter-arrival time, which for Central Texas is around 5 days [68], while for Duke Forest it averages about 3 days (hence, $T = 25$ and 15 days respectively). For all species a mean rooting depth of 0.3 m, a soil porosity of 0.45, and initial soil moisture around the soil field capacity (here taken as $x_0 = 0.8$) were assumed. Day length was set to 12 h and a factor of 2/3 was used to reduce the light-saturated photosynthetic rate to approximately account for the daily light cycle. The numerical values of λ for the herbaceous species have been estimated through linear regression using the relation linking photosynthesis, the square root of stomatal conductance, and λ [48], whereas λ for *P. taeda* was obtained from published results employing a similar regression approach [64].

The effect of soil moisture limitations was assessed using data for *Nerium oleander* grown in pots in controlled conditions ($D = 0.01$ mol mol^{-1}, $c_a = 300$ μmol mol^{-1}) and subjected to a prolonged dry-down [66]. Carboxylation capacity was estimated from reported A-c_i data, but because supplemental light was provided it was not corrected for the daily light cycle. For this study we assumed $T = 20$ d and $Z_r = 0.1$ m to reflect the limited soil volume available in the pots; no competition occurred because individual plants were planted in each pot. No specific information on total leaf area, plant density, and root development were provided, so we performed Monte Carlo simulations to estimate confidence intervals for the optimal solutions that accounted for uncertainty in LAI and k_{SR}. Parameters were extracted from independent normal distributions with given mean and standard deviations. We extracted 1000 values of LAI and k_{SR}, computed the corresponding initial Lagrange multipliers, and calculated the optimal stomatal conductance and photosynthesis as a function of soil moisture for each realization. The obtained percentiles for each soil moisture bin stabilized above 500 realizations, giving confidence that the chosen number of extractions was sufficiently large. Using initial Lagrange multipliers obtained from the Monte Carlo simulation under growth conditions ($D = 0.01$ mol mol^{-1}), stomatal conductance and photosynthesis were also computed for $D = 0.025$ mol mol^{-1} and compared to the observations.

Uncertainties in the parameter estimation approach prevented us from providing a rigorous validation. However, in all model-data

Table 2
Summary of optimal solutions for different terminal conditions and water loss functions.

Soil moisture limitation	Terminal state, $x(T)$	Uncontrolled losses	Terminal gain, J_T	Optimal stomatal conductance, $g_{opt}(t)$	Lagrange multiplier, $\lambda(t)$	Initial value of the Lagrange multiplier, λ_0	Optimal soil moisture, $x(t)$
No soil moisture limitation; g is a free control variable	0[a]	$\beta \geqslant 0$, $c = 0$	0	$k\left(\sqrt{\frac{c_a}{\alpha D \lambda_0}} - 1\right)$	λ_0	$c_a \alpha D \left(\frac{x_0 - \beta T}{kT} + \alpha D\right)^{-2}$	$x_0 - (\beta + \alpha g_{opt} D)\, t$
	0[a]	$\beta \geqslant 0$, $c = 1$	0	$k\left(\sqrt{\frac{c_a}{\alpha D \lambda_0 e^{\beta t}}} - 1\right)$	$\lambda_0 e^{\beta t}$	$\frac{4 c_a k^2 (1 + e^{\beta T} - 2\sqrt{e^{\beta T}})}{[(e^{\beta T} - 1) k \alpha D + \beta x_0]^2}$	$\frac{k}{\beta} e^{-\beta t}\left[\frac{x_0 \beta}{k} + \alpha D (e^{\beta t} - 1) + 2\sqrt{\frac{\alpha D c_a}{\lambda_0}}\left(e^{\frac{\beta t}{2}} - 1\right)\right]$
	Free ($x > 0$)[b]	$\beta \geqslant 0$, $c = 1$	Λx	$k\left(\sqrt{\frac{c_a}{\alpha D \Lambda e^{\beta(t-T)}}} - 1\right)$	$\Lambda e^{\beta(t-T)}$	$\Lambda e^{-\beta T}$	$\frac{k}{\beta} e^{-\beta t}\left[\frac{x_0 \beta}{k} + \alpha D (e^{\beta t} - 1) + 2\sqrt{\frac{\alpha D c_a}{\lambda_0}}\left(e^{\frac{\beta t}{2}} - 1\right)\right]$
Soil moisture-limited regime; g and x are constrained (subscript 'b')	0[a]	$\beta \geqslant 0$, $c = 0$	0	$g_b(x_b) = \frac{k_{SR}}{v a D} x_b(t)$	Equation (8)	Numerical solution of $x(T) = 0$	$x_b(t) = \frac{\beta}{\kappa}[e^{(t^* - t)\kappa} - 1] + x^* e^{(t^* - t)\kappa}$[c]
	$\chi\, x_0$[a,d]	$\beta \geqslant 0$, $c = 1$	0	$g_b(x_b) = \frac{k_{SR}}{v a D} x_b(t)$	Equation (8)	Numerical solution of $x(T) = \chi\, x_0$	$x_b(t) = x^* e^{(t^* - t)(\beta + \kappa)}$[c]

[a] Referred to as *intensive* water use strategies.
[b] Referred to as *conservative* water use strategies.
[c] The transition time to the soil moisture-limited range, t^*, is obtained from the condition $g_{opt}(t^*) = g_b[x(t^*)]$; the corresponding soil moisture level, x^*, is computed as $x^* = x_{opt}(t^*)$. Analytical expressions for t^* and x^* are not reported for conciseness.
[d] The exponential form of the constrained soil moisture trajectory does not allow fully depleting soil moisture; hence, a higher soil moisture threshold is introduced and defined as a fraction χ of the initial moisture value.

Table 3
Parameter values for all the species considered. Values in parentheses indicate the standard deviation of the normal distributions employed in the Monte Carlo simulations in Fig. 8.

Parameter	Units	Species			
		S. canadensis	*S. nutans*	*P. taeda*	*N. oleander*
γ	m d^{-1}	½E_{pot}	½E_{pot}	¼E_{pot}	0
D	mol mol^{-1}	0.03	0.03	0.015	0.01–0.025[a]
E_{pot}	m d^{-1}	0.006	0.006	0.005	–
k	mol m^{-2} s^{-1}	0.024	0.072	0.051	0.1
k_{SR}	m d^{-1}	Not limiting	Not limiting	Not limiting	0.008 (0.004)
LAI	m^2 m^{-2}	1.5	1.5	4	2 (0.5)
T	d	25	25	15	20
x_0	m^3 m^{-3}	0.8	0.8	0.8	1
Z_R	m	0.3	0.3	0.3	0.1

[a] Vapor pressure deficit respectively during growth (for which the plants is assumed to be optimized) and during a separate set of short-term measurements.

comparisons the reported data points were not used to calibrate the model, but were independent observations, thus illustrating the model potential to capture observed patterns.

3. Results and discussion

In Section 3.1, simplified cases are considered to derive analytical solutions of the stomatal optimization problem presented in Section 2.1 (a summary of the analytical solutions is reported in Table 2). The simplest case of constant soil moisture (and undetermined λ) is considered first, followed by cases where soil moisture is allowed to vary through time (variable λ), including different formulations for the uncontrolled water losses and the final gain J_T, and soil moisture limitations on transpiration. Section 3.2 compares the theoretical predictions to observations and generalizations of the proposed models are discussed in Section 3.3.

3.1. Particular solutions for the optimization problem

3.1.1. Constant soil moisture

If soil moisture variations are small so that they can be neglected over the time interval T (a reasonable approximation when T is about a day), Eq. (2) reduces to $x(t) \approx x_0$. Without the dynamic constraint of Eq. (2), soil moisture does not affect the Hamiltonian, so that $d\lambda/dt = 0$ (from Eq. (5)), i.e., λ remains constant through time, denoted by λ_0. In this case, the only necessary optimality condition to be fulfilled is provided by Eq. (4), which leads to the definition of a constant optimal stomatal conductance. Using Eqs. (9) and (10), the Hamiltonian can be written as (from Eq. (3))

$$H = \frac{g\, c_a k}{g + k} - \lambda_0 \frac{v a g D + L}{n Z_r}. \tag{14}$$

Differentiating H with respect to g and equating to zero (Eq. (4)), an expression for optimal stomatal conductance as a function of environmental parameters (D and c_a) and the (constant) Lagrange multiplier (λ_0) is found as

$$g_{opt}(t) = k\left(\sqrt{\frac{c_a}{\alpha D \lambda_0}} - 1\right), \tag{15}$$

where the constant $\alpha = va(nZ_r)^{-1}$ and the optimal solution is indicated by subscript '*opt*'. Variations of g_{opt} through time are only caused by changes in the environmental drivers D, c_a and light (assuming light affects the value of k), but are not due to changes in the Lagrange multiplier.

Eq. (15) and its variants including a nonlinear $A(c_i)$ curve and atmospheric resistance have been derived following different approaches in numerous publications [30,47,56,57,64,69]. Due to the lack of a second necessary condition for optimality, however, Eq. (15) is not mathematically closed, and λ_0 needs to be estimated from observed gas exchange rates [45,46]. This optimality solution has been found to correctly predict observed relationships between gas-exchange rates and environmental variables when soil moisture is non-limiting, namely:

1. The scaling between stomatal conductance and vapor pressure deficit at a given light availability and moderate D, $g \propto D^{-1/2}$ [45,47,57,70];
2. The scaling between photosynthesis and stomatal conductance for a given atmospheric CO_2 concentration, $A \propto g \times D^{1/2}$, as can be demonstrated by combining Eqs. (10) and (15) [39,48,71–73].
3. The apparent feed-forward mechanism that implies a negative sensitivity of transpiration to vapor pressure deficit in dry conditions [47,74]: using Eq. (15), $\partial E/\partial D \propto [c_a/(4\alpha\lambda_0)]^{1/2} D^{-1/2} - 1$ is positive for small D, crosses zero at a fixed $D = c_a/(4\alpha\lambda_o)$, and becomes negative thereafter.

However, when λ_0 is held constant, Eq. (15) predicts larger stomatal conductance as atmospheric CO_2 is increased, contrary to most observations [75,76] and does not include the effect of soil moisture on stomatal conductance. This lack of sensitivity led to empirical 'corrections' that modify λ_0 with atmospheric CO_2 concentration and soil moisture to match gas exchange data [53,58,64]. Both CO_2 and water limitations as well as the formulations used in these closure models can be addressed by accounting for soil moisture dynamics in this optimization framework, as described next.

3.1.2. Variable soil moisture with intensive water use

The dynamic constraint expressed by the soil water balance (Eq. (2)) is now explicitly considered with reference to a single prolonged dry-down of duration T during which no rain occurs. Soil moisture is depleted starting from an initial value x_0, which will be assumed close to the field capacity. The dry-down duration is interpreted as about five times the mean interval between two rainfall events, representing a hydro-climatic time scale for a complete dry-down of the location under consideration. This deterministic value of T was selected to illustrate the optimal trajectories over a wide range of soil moisture values (generalizations to stochastic rainfall are discussed in Section 3.3.1). For plants that can be considered intensive water users, it is also assumed that all the available water is exploited by the end of the dry-down period, so that $x(T) = 0$. In this case, a logical assumption is that the objective of the plant is to maximize the cumulative C uptake during the interval T (Eq. (1)) with no consideration to the end-condition, i.e., the terminal C gain is neglected (this assumption is relaxed in Section 3.1.4).

Using the simplified gas exchange model in Eqs. (9) and (10) and Eq. (11), the soil moisture balance equation during a dry-down becomes

$$\frac{dx}{dt} = -\alpha g D - \beta x^c, \tag{16}$$

where $\alpha = va(nZ_r)^{-1}$, $\beta = \gamma(nZ_r)^{-1}$, and D represents an average vapor pressure deficit during the dry period. The Hamiltonian (from Eq. (3)) is now given by

$$H = \frac{g\, c_a k}{g + k} - \lambda(t)(\alpha g D + \beta x^c), \tag{17}$$

where c_a and k are also interpreted as time-averaged quantities. The first condition for optimality (Eq. (4)) can be solved to obtain optimal stomatal conductance as a function of the Lagrange multiplier λ,

$$g_{opt}(t) = k\left(\sqrt{\frac{c_a}{\alpha\lambda(t) D}} - 1\right), \tag{18}$$

which is formally identical to Eq. (15), except that now g_{opt} changes in time due to both fluctuations in the environmental drivers and variations in λ. This outcome is more general than the previous condition described elsewhere where it was shown that the canonical form of the optimal solution is maintained for a variable $\lambda(t)$ provided $|\partial\lambda/\lambda| \ll |\partial g/g|$ [47].

The temporal evolution of λ is now provided by solving Eq. (5),

$$\frac{d\lambda}{dt} = -\frac{\partial H}{\partial x} = \beta\lambda(t) c x^{c-1}, \tag{19}$$

with initial condition $\lambda(0) = \lambda_0$ still to be determined. It is important to emphasize that the terminal condition for the Lagrange multiplier is free because the terminal gain has been neglected, while the initial value of the multiplier can be determined by imposing the condition that all water is used by the end of the dry period, i.e., $x(T) = 0$ [16]. In the following, two cases are considered: water losses not controlled by plants are independent of soil moisture ($c = 0$ in Eq. (11)) and linearly related to soil moisture ($c = 1$; these formulations are respectively indicated by dotted and solid lines in Figs. 1–5).

In the first case of uncontrolled losses independent of soil moisture ($c = 0$), Eq. (19) yields a time-invariant $\lambda(t) = \lambda(0) = \lambda_0$. In this case, g_{opt} is also constant, so that the soil moisture balance can be solved as

$$x(t) = x_0 - (\beta + \alpha g_{opt} D) t, \tag{20}$$

that is, a linear decline of soil moisture in time is predicted. Imposing the condition $x(T) = 0$, the value of λ_0 can be obtained,

$$\lambda_0 = c_a \alpha D \left(\frac{x_0 - \beta T}{kT} + \alpha D\right)^{-2}, \tag{21}$$

which mathematically closes the problem (Table 2). Sample trajectories of g_{opt}, λ, and x over a single dry-down are shown in Fig. 1 (dotted lines). Because λ_0 is constant during the dry period, also the optimal stomatal conductance remains constant. Accordingly, plants transpire at a constant rate until the available soil water is completely depleted, similar to the formulations employed by Milly [77] and Guswa [9] in their stochastic eco-hydrological models. It is important to emphasize that λ_0 in Eq. (21) depends on the *average* environmental parameters experienced by the plant during the dry-down; however, environmental fluctuations around these averages affect the instantaneous optimal stomatal conductance (Eq. (18)).

The effects on λ_0 of average atmospheric CO_2 concentration and dry period length are explored in Figs. 2 and 3, respectively. Using this simple model, λ_0 scales linearly with atmospheric CO_2 concentration (dotted line in Fig. 2(A)), consistent with previous studies that evaluated λ_0 based on observations [58,64,72,78]. As a result of this linear relation, however, the model predicts that c_a should not have any effect on stomatal conductance (dotted line in Fig. 2(B)), whereas a decrease in stomatal conductance has typically been observed under elevated CO_2 concentrations. The value of λ_0 also increases with increasing duration of the dry down (Fig. 3(A)) and increasing vapor pressure deficit, implying that growing in dry conditions decreases stomatal conductance (dotted lines in Figs. 3(B) and 4). This result is consistent with observations of slower water consumption in more arid ecosystems, at least in perennial species. In the second case, assuming uncontrolled losses are linearly dependent on soil moisture ($c = 1$), Eq. (19) provides the following time-varying $\lambda(t)$ (solid line in Fig. 1(B)),

$$\lambda = \lambda_0 e^{\beta t}. \tag{22}$$

Because $\beta = \gamma/(nZ_r) > 0$, λ exponentially increases through time (as the available water declines). As a consequence, optimal stomatal conductance now decreases as the drought progresses (from Eq. (18); Fig. 1(A), solid line),

$$g_{opt}(t) = k\left(\sqrt{\frac{c_a}{\alpha D \lambda_0 e^{\beta t}}} - 1\right). \tag{23}$$

Accordingly, solving Eq. (16), soil moisture follows a declining exponential trajectory (Fig. 1(C), solid line),

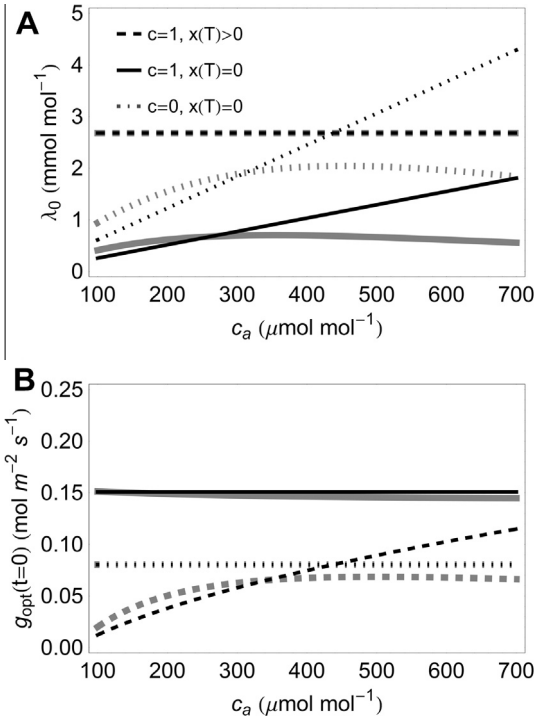

Fig. 2. Effects of atmospheric CO_2 concentration (c_a) on (A) the initial value of the Lagrange multiplier (λ_0) and (B) the initial optimal soil moisture (g_{opt}). Thick gray lines refer to solutions obtained for the nonlinear $A(c_i)$ curve (Appendix C; note that g_{opt} for the two models is the same for $c = 0$). Line dashing and parameters other than c_a are as in Fig. 1; in the nonlinear model, kinetic parameters were chosen to have under ambient c_a a carboxylation efficiency comparable to the value of k used in the linear model (a_1 = 35 mol m^{-2} s^{-1}, a_2 = 400 μmol mol^{-1}).

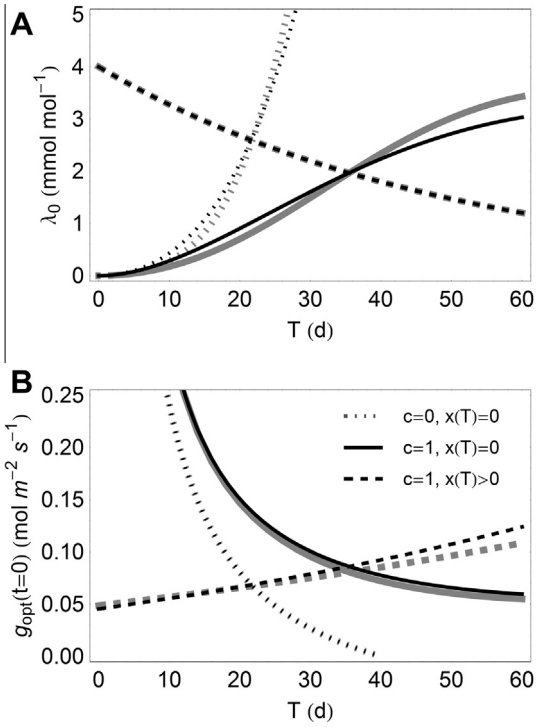

Fig. 3. Effects of dry-down duration (T) on (A) the initial value of the Lagrange multiplier (λ_0) and (B) the initial optimal soil moisture (g_{opt}). Thick gray lines refer to solutions obtained for the nonlinear $A(c_i)$ curve (Appendix C; note that g_{opt} for the two models is the same for $c = 0$). Line dashing and parameters other than T are as in Figs. 1 and 2.

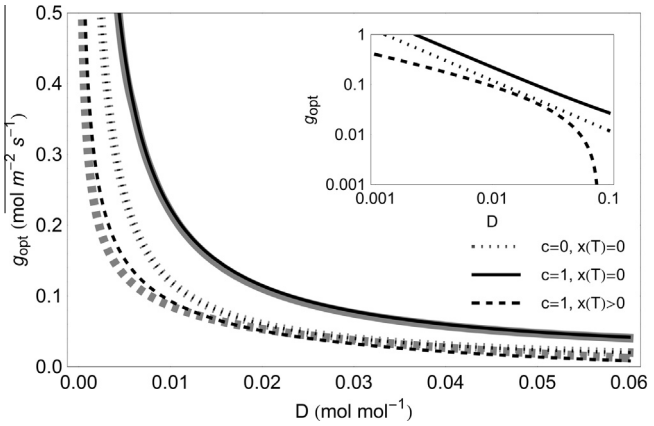

Fig. 4. Effect of vapor pressure deficit (D) on optimal stomatal conductance (g_{opt}), for different optimization schemes (line dashing as in Fig. 1) and under well-watered conditions. The inset shows the same curves, but in logarithmic scale to distinguish the different behaviors at high D. Thick gray lines refer to solutions obtained for the nonlinear $A(c_i)$ curve (Appendix C) Parameters other than D are as in Figs. 1 and 2.

$$x(t) = \frac{k}{\beta} e^{-\beta t}\left[\frac{x_0\beta}{k} + \alpha D(e^{\beta t} - 1) + 2\sqrt{\frac{\alpha D c_a}{\lambda_0}}\left(\sqrt{e^{\beta t}} - 1\right)\right], \tag{24}$$

which is consistent with observations (e.g., [5,65]). As before, by setting $x(T) = 0$, the numerical value of the initial Lagrange multiplier λ_0 can be determined (Table 2),

$$\lambda_0 = 4c_a k^2 \frac{1 + e^{\beta T} - 2\sqrt{e^{\beta T}}}{(e^{\beta T} - 1)k + \beta x_0 (\alpha D)^{-1}}. \tag{25}$$

The λ_0 increases linearly with atmospheric CO_2 concentration, as in the case of uncontrolled losses independent of soil moisture (solid line in Fig. 2(A)) yielding the same unrealistic response of stomatal conductance (solid line in Fig. 2(B)). However, when using the nonlinear $A(c_i)$ curve (Appendix C), λ_0 is found to increase moderately with c_a, reaching a plateau around current ambient CO_2 concentration (solid gray line in Fig. 2(A)). This pattern in λ corresponds to slightly decreasing optimal stomatal conductance throughout the selected range of atmospheric CO_2 concentrations (Fig. 2(B)), but this decline is smaller than in most observations.

The value of λ_0 also increases as the length of the dry period increases. This pattern may be interpreted as a shift in water use towards more conservative strategies (low conductance and high λ_0) as the expected dry period becomes longer (Fig. 3(A), solid line). Moreover, for a fixed β (as in Figs. 1–4), the water losses under well-watered conditions are the same for $c = 0$ or 1, but in the former case they remain constant as soil moisture decreases, whereas in the latter water losses decline linearly as the soil dries. As a consequence, when $c = 1$ the contribution of transpiration to the soil water balance is larger and λ is expected to be correspondingly lower (compare solid and dotted lines in Fig. 1). Similar to the previous case, also dryer air (high D) causes lower stomatal conductance at a given soil moisture (solid lines in Fig. 4).

By combining Eqs. (22) and (24), it is possible to link λ to soil moisture through the implicit equation,

$$x = \frac{k}{\beta}\frac{\lambda_0}{\lambda}\left[\frac{x_0\beta}{k} + \alpha D\left(\frac{\lambda}{\lambda_0} - 1\right) + 2\sqrt{\frac{\alpha D c_a}{\lambda_0}}\left(1 - \sqrt{\frac{\lambda}{\lambda_0}}\right)\right], \tag{26}$$

which has an analytical (but cumbersome) solution $\lambda(x)$ that we do not report for conciseness. Fig. 5 illustrates this relation by plotting λ and soil moisture as time progresses during a dry down, for two dry-down durations (solid lines). The result that λ increases as x decreases is consistent with previous theoretical studies [43,44,49,79],

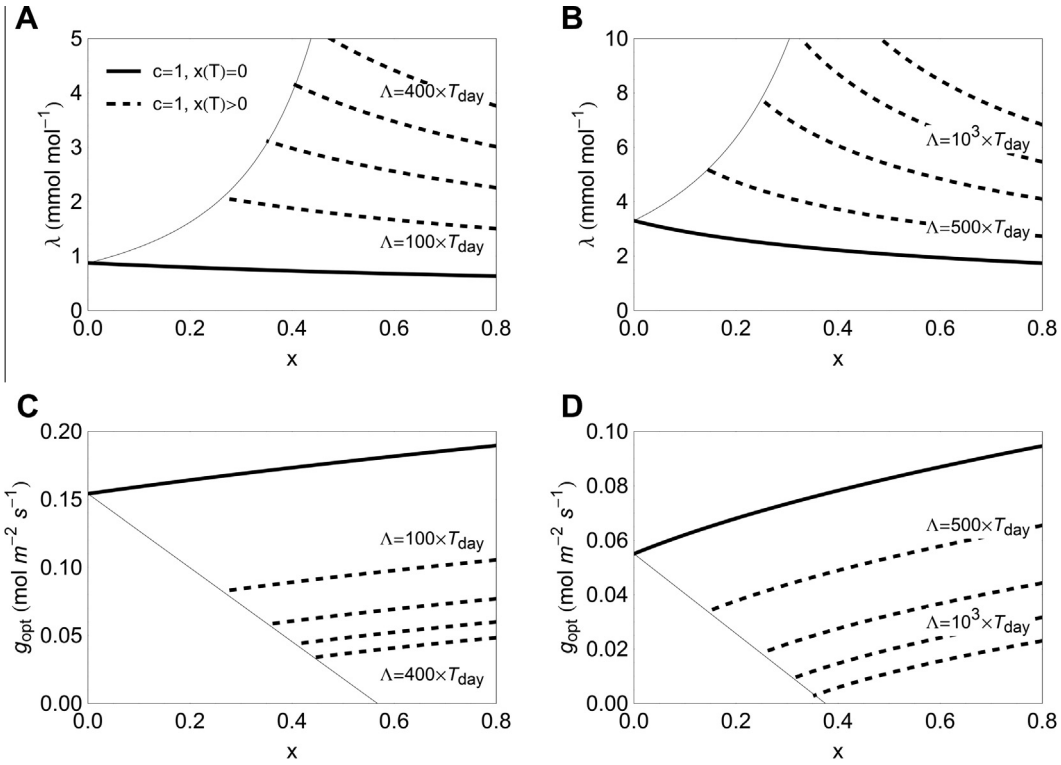

Fig. 5. Lagrange multiplier (λ, upper panels) and optimal stomatal conductance (g_{opt}, lower panels) as a function of soil moisture (time progresses from right to left, as x is depleted). Left panels: short dry-down of duration of $T = 16$ d; right panels: long dry-down of duration of $T = 32$ d (note the different range on the ordinate axes). Line style denotes different optimization formulations, as in Fig. 1; for the case of non-zero terminal gain, several trajectories are shown for different values of Λ (in μmol m^{-2}). The thin solid lines are the envelopes of the terminal states for different choices of Λ (i.e., the minimum theoretical soil moisture, $x(T)$); other parameter values are as in Fig. 1.

semi-empirical formulations linking λ to soil moisture [51,52,80], and empirical estimates of λ [53,58,81].

3.1.3. Effect of soil moisture limitation on transpiration

The optimal time trajectories of stomatal conductance and soil moisture are now computed when transpiration may become soil moisture-limited, for both formulations for the uncontrolled losses ($c = 0$ and $c = 1$). The transition time t^* between the free and soil moisture-limited regimes can be obtained by setting $g_{opt}(t^*) = g_b[x(t^*)]$, corresponding to the soil moisture threshold $x^* = g_{opt}(t^*)\, vaD/k_{SR}$ (from Eq. (13)). It is important to emphasize that the thresholds t^* and x^* are both dependent on the initial value of the Lagrange multiplier, which remains undetermined until a condition on the final state of the system is imposed. When the system reaches the soil moisture-limited regime, both soil moisture and stomatal conductance are constrained (Eq. (13)), and the soil moisture equation reads

$$\frac{dx}{dt} = -\alpha g_b D - \beta x^c = -\kappa x - \beta x^c, \tag{27}$$

where $\kappa = k_{SR}(nZ_r)^{-1}$. Eq. (27) can be solved for $c = 0$ or $c = 1$ to obtain $g_b(t)$ (Table 2), and the constrained stomatal conductance is accordingly found as $g_b = k_{SR}/(vaD)x_b = \kappa/(\alpha D)x_b$. Setting a condition for the final soil moisture (here $x(T) = x_0/100$) allows finding λ_0 without determining the whole temporal trajectory of λ. In problems where a final gain is present or no final condition is imposed on x, the final condition of λ is known and λ_0 can only be found by integrating Eq. (8). We do not discuss these cases here for conciseness.

Fig. 6 shows how the optimal stomatal conductance and the Lagrange multiplier change as a function of soil moisture and for different hydraulic properties of the soil-root system, for linear uncontrolled losses ($c = 1$). When water transport in the root zone is inhibited by low conductivity or small root area (low k_{SR}), the soil moisture-limitations to transpiration become apparent (Fig. 6(A)). Stomatal conductance decreases more sharply with soil moisture than without limitations as it becomes constrained by water supply (compare to Fig. 5), while lower values of k_{SR} cause larger g_{opt} in well-watered conditions to compensate for the lowered water use later in the dry-down. The Lagrange multiplier follows a pattern similar to the previous cases until the transition to soil moisture limitation is reached (Fig. 6(B)). Beyond that threshold, however, λ decreases sharply. This decrease is shown here for completeness, but it cannot be readily interpreted from a physical or biological perspective. In fact, λ is equivalent to the marginal water use efficiency when moisture is not limiting (as can be inferred from Eq. (4)), but under moisture limitation λ takes a different trajectory due to the added constraint (Eq. (6)). This difference is highlighted in Fig. 6(B), where the Lagrange multiplier peaks around the transition point to the soil moisture-limited regime, whereas the marginal water use efficiency keeps increasing under moisture limitation. This sharp increase of the marginal water use efficiency when water availability declines is consistent with observations [58] and previous theoretical works [43,49,51,79]. The stomatal conductance-soil moisture relations, with the sharp transition between the two regimes (Fig. 6(D)), also resemble observed patterns [66,82,83] and are consistent with frequently-used empirical models of transpiration [5].

3.1.4. Variable soil moisture with conservative water use (terminal gain)

Maintaining some water at the end of an 'average' dry-down could be advantageous to avoid the consequences of water stress (not implemented explicitly thus far in previous studies) and improve C uptake after rainfall and during the following dry periods.

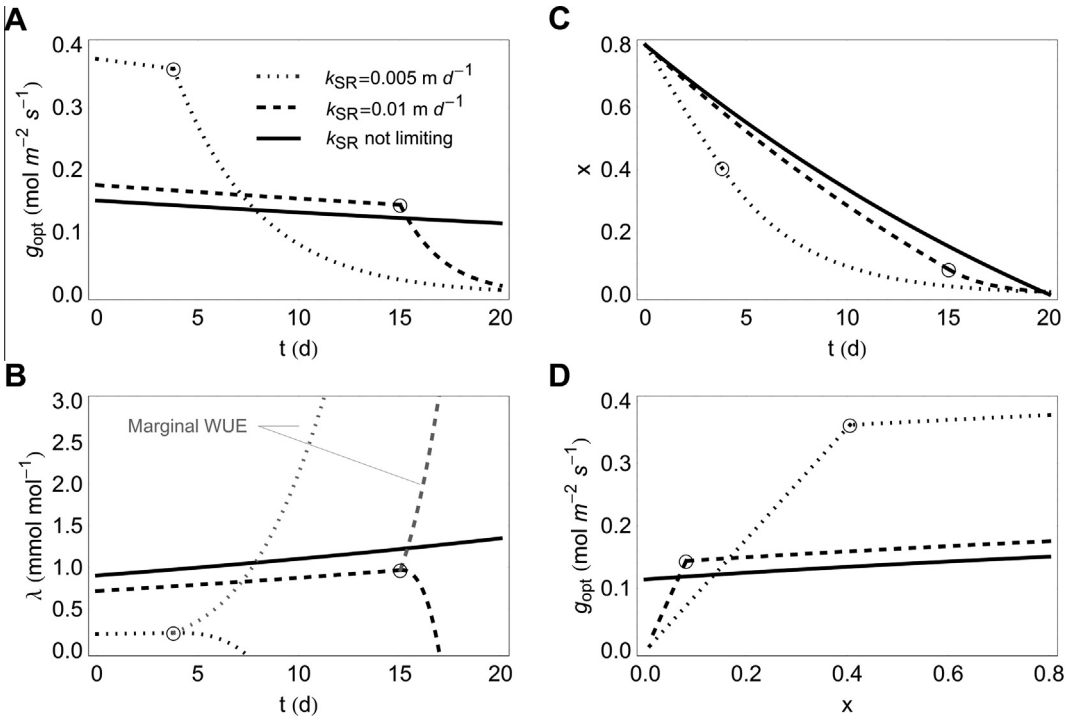

Fig. 6. Effect of soil moisture limitation on the temporal evolution of (A) optimal stomatal conductance, (B) the Lagrange multiplier, (C) soil moisture, and (D) on the stomatal conductance-soil moisture relation (all curves refer to the case $c = 1$). Solid lines indicate trajectories not affected by soil moisture limitation (as in Figs. 1 and 4); dashed and dotted lines refer to increasingly severe soil moisture limitation (i.e., decreasing k_{SR}). The transition to the moisture-limited regime is marked by circles. Gray lines in B) show the temporal changes in marginal water use efficiency (WUE), to emphasize the divergence from $\lambda(t)$ for $t > t^*$. $T = 20$ d, $\chi = 0.01$, and other parameter values are as in Fig. 1.

For instance, it could be advantageous to save soil water to avoid cavitation and the associated C costs for the refilling of embolized xylem conduits [84], avoid metabolic limitations to photosynthesis [54], and limit the need to shed part of the foliage in response to drought [42]. Avoiding these costs corresponds to a net C gain that increases with the amount of soil moisture remaining at the end of the dry period. The simplest approach to capture this strategy is to assume that the terminal gain is proportional to the remaining plant-available water at the end of the dry-down via

$$J_T = \Lambda x(T), \tag{28}$$

where Λ is a factor expressed in terms of C mass per unit ground area. Including the terminal C gain in the objective function (Eq. (1)) alters the boundary condition of the differential equation for $\lambda(t)$. It can be shown that when a terminal gain is present in a fixed terminal time optimization, the final state of the Lagrange multiplier is given by $\lambda(T) = \partial J_T/\partial x|_{x=x(T)}$ [16,55]. Using the formulation in Eq. (30) and assuming linear dependence of uncontrolled losses on soil moisture ($c = 1$), Eq. (19) can be analytically solved to yield (dashed line in Fig. 1(B))

$$\lambda = \Lambda e^{\beta(t-T)}. \tag{29}$$

Accordingly, optimal stomatal conductance can be determined from Eq. (20) as,

$$g_{opt}(t) = k\left(\sqrt{\frac{c_a}{\alpha D \Lambda e^{\beta(t-T)}}} - 1\right), \tag{30}$$

in which g_{opt} declines during the dry periods due to changes in λ (dashed line in Fig. 1(A)). The only difference between this formulation and the one constrained to $x(T) = 0$ (Section 3.1.2) is the temporal dependence of the Lagrange multiplier and its initial value. Unlike Eq. (23), where the Lagrange multiplier did not embed any information on the final state of the soil–plant system, here the parameter Λ is a measure of how 'advantageous' a conservative water use strategy is in C units. While the current formulation does not explicitly link Λ to measurable stress response C costs, the value of this parameter may be used to link the long-term plant C economy to optimal gas exchange at the scale of the dry-down. Furthermore, it can be shown that Eq. (26) still holds in this case, after imposing that $\lambda_0 = \Lambda e^{-\beta T}$ (from Eq. (29)). Because in this case λ only depends on the terminal gain and the duration of the dry period (and is independent of c_a and D; Fig. 2), stomatal conductance unrealistically increases with c_a.

The conservative water use strategy shows a qualitatively different behavior when compared to the other models, because the amount of water that is used is 'adjusted' to optimally balance C gains during and at the end of the dry-down. As a consequence, according to this strategy, it becomes more convenient to use water faster as the dry-down lengthens, because the contribution of the final condition decreases compared to the C gain that is accumulated during the period T. This seemingly counterintuitive pattern is shown in Fig. 3 (dashed lines). Notably, if the final gain Λ is increased as a function of T, the pattern could be reversed, obtaining a decrease in optimal stomatal conductance as T increases.

As illustrated in Fig. 4, the sensitivity of stomatal conductance to vapor pressure deficit for this formulation is lower at low D and higher at large D than in the previous models (dashed *vs.* solid and dotted lines in Fig. 4). Fig. 5 shows how λ and g change as a function of soil moisture for different values of the terminal gain parameter λ Terminal gains comparable to the total C uptake obtained over the duration T of the dry-down are sufficient to introduce significant deviations in the predicted optimal conductance trajectories, with respect to the case of intensive water use. Larger gains at the end of the dry-down and longer dry intervals cause steeper increases in the function $\lambda(t)$ as soil moisture decreases, consistent with empirical findings [58] (see also Section 3.2). However, even with large terminal gains, the predicted trajectories for λ

tend to increase less steeply than previous leaf-level estimates [58], suggesting that soil moisture limitations might need to be accounted for (Section 3.1.3; see also the discussion in Section 3.3.2).

3.2. Evaluation of theoretical predictions using existing datasets

Stomatal optimization theories based on the assumption of constant soil moisture and constant marginal water use efficiency (Eq. (15)) have been tested in various conditions (see Section 3.1.1). However, estimated λ has been found to vary when water availability is changed. This variability has been interpreted as proof that stomatal behavior is not optimal [85–87], while we show that changes in λ can be consistent with optimality under certain constraints. In this section, theoretical predictions of the relation between λ and atmospheric CO_2, and between optimal gas exchange rates and soil moisture are compared with empirical evidence.

The predicted λ_0 for linear uncontrolled water losses (i.e., $c = 1$ and Eq. (25)) are compared to empirically estimated values in Fig. 7. The agreement between theory and data is encouraging, also considering the large variability in the estimated marginal water use efficiency and the uncertainties in the parameters of Eq. (25). The assumption that all plant-available soil water is used at any c_a level implies that the optimal stomatal conductance is constant with respect to c_a. This lack of down-regulation is inconsistent with some observations [75,76], indicating that either the assumption of constant carboxylation capacity needs to be relaxed, or that this minimal formulation of the optimization problem might oversimplify the feedbacks driving plant gas exchange (as discussed in Section 3.3.3). Despite this lack of sensitivity, the predicted g is close to the observations in *P. taeda*, while it is slightly overestimated and underestimated in *S. nutans* and *S. canadensis*, respectively. Photosynthesis is instead in better agreement with observations for all species. In contrast to this linear scaling, when a terminal gain is considered, λ is predicted to be independent of c_a (Table 2). We surmise that an intermediate water use strategy could be expected, explaining the less-than-linear increase of the λ–c_a relation that appears for *S. canadensis* and *P. taeda* in Fig. 7. A similarly invariant λ with increasing CO_2 concentration is found when the $A(c_i)$ function is curvilinear instead of linear, as would be the case under light limitation [73,88].

The effects of soil moisture on stomatal conductance and photosynthesis are explored in Fig. 8, where two sets of gas exchange data are considered: growth conditions (lower VPD, open symbols) and altered conditions during measurement (high VPD, closed symbols). For this analysis we selected the solutions for linear uncontrolled losses ($c = 1$) and complete depletion of soil water with the inclusion of soil moisture limitations (Table 2). The model is able to predict the observations under both conditions within 95% confidence intervals, when accounting for uncertainty in two parameters, LAI and the coefficient characterizing water supply to the roots, k_{SR}. With the chosen parameter values and variability, the model predicts gas exchange under growth conditions better than it does under altered conditions, where it tends to underestimate g and A. In both cases, however, the model predicts a sharp decline of gas exchange rates as soil moisture becomes limiting, as also apparent from the data.

While a more rigorous validation of the proposed theory is warranted, this uncertainty analysis suggests that, despite its simplicity, the theory is sufficiently flexible to capture observed relations between stomatal conductance and photosynthesis, and soil moisture. One of the most important parameters to characterize the soil moisture-limited regime, k_{SR}, is also among the most uncertain, as it accounts for both soil (hydraulic conductivity) and root properties (root area density and geometry) that are not readily measured in typical drought response studies. Also from a theoretical perspective, determining k_{SR} from measurable parameters is not simple, because the microscopic features of the root system are in general not known and thus the definition of a macroscopic parameter such as k_{SR} may be problematic and requires *a priori* assumptions on the specific geometry of the root system [61,89,90].

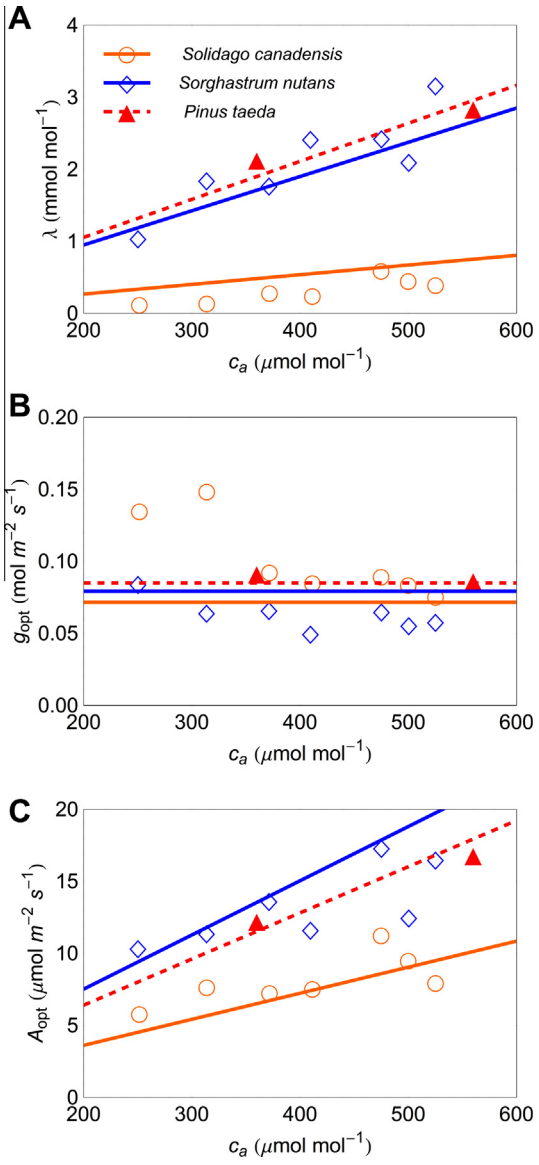

Fig. 7. Predicted and observed effect of atmospheric CO_2 concentration, c_a, on (A) Lagrange multiplier, λ_0, (B) optimal stomatal conductance, g_{opt}, and (C) optimal photosynthesis, A_{opt}, in three contrasting species (a C_3 herb, *S. Canadensis*; a C_4 grass, *S. nutans*; a conifer tree, *P. taeda*) grown under different c_a. The optimal solutions are obtained assuming linear uncontrolled losses (Eqs. (23) and (25)); λ_0 values and other parameters have been estimated as described in Section 2.5 (see also Table 3).

3.3. Future developments

3.3.1. Stochastic approaches

Accounting for the randomness of rainfall events (in terms of their timing and amounts) is the most natural extension of the optimization framework described here. Random rainfall inputs create a distribution of initial soil moisture states and dry-down durations that complicate the formulation of the optimal control problem. Moreover, each dry-down is connected to the previous ones through the dynamic changes of soil moisture and rainfall.

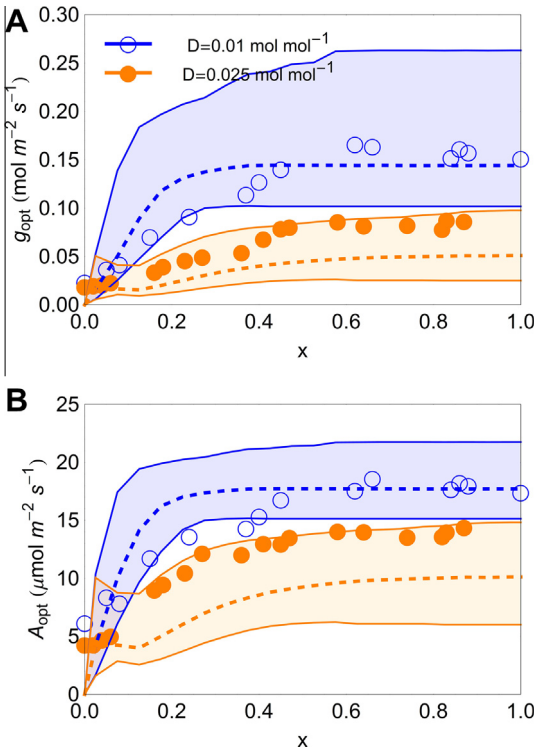

Fig. 8. Effect of soil moisture, x, on (A) optimal stomatal conductance, g_{opt}, and (B) optimal photosynthesis, A_{opt}, in *N. oleander* grown at $D = 0.01$ mol mol^{-1}, but sampled also at $D = 0.025$ mol mol^{-1} (data from [66]). Dashed and solid lines respectively indicate median and 95% confidence intervals based on Monte Carlo simulations to assess the role of variability in LAI and k_{SR}. Values of λ_0 and other parameters have been estimated as described in Section 2.5 (see also Table 3).

Optimizing stomatal conductance to maximize C uptake during any sequence of drying-wetting events would become rapidly unmanageable.

A more meaningful objective function to be maximized under stochastic conditions, in which rain inter-arrival times and depths are variable, would be the long-term mean C uptake, rather than the total uptake realized over a period of finite duration [9,15,43,44,79,91,92]. Alternatively, the long-term mean water stress could be minimized, assuming that productivity is inversely related to the occurrence of water stress events [29,93,94]. Rainfall events may be described as a Poisson process where the duration of dry periods (here assumed constant through the parameter T) follows an exponential distribution [2,5,43,77]. Using this approximation, and further assuming that all rainfall events restore saturated conditions, λ has been shown to increase as drought conditions worsen [43,79]. The model by Cowan [43] considers competition for water with physical water losses and water-stress mortality risk as the main drivers of stomatal closure, and λ is determined such that the mean photosynthesis is maximized, provided that soil water is not completely depleted during a drought. Mäkelä et al. [79] found that λ increases exponentially in time during a dry period, but they neglected uncontrolled water losses and the fact that during each dry period of random duration a different amount of water is lost from the soil. The only approach that also accounts for stochastic rainfall depths was proposed by Cowan [44], but his derivation was not complete [4].

3.3.2. Metabolic and hydraulic limitations

The theory presented here neglects the feedbacks of stomatal conductance on leaf water potentials and photosynthetic capacity. As soil dries, the water supply to the leaves decreases; if stomata do not close in response to such changes in supply, the leaf water potential may decline to levels that inhibit photosynthetic efficiency [53,54,95]. Albeit less evident than at the leaf scale, these metabolic limitations appear also at the whole canopy level under severe stress (e.g., [96]). This feedback causes the carboxylation efficiency to decrease as water stress progresses, such that $\partial A/\partial g$ may become even negative if stomata remain open. Based on this principle, Williams et al. [97] defined the optimal stomatal conductance as the point where $\partial A/\partial g = 0$, but did not frame this modeling assumption as an optimal control problem. Including the negative effect of leaf water potential on photosynthesis has been shown to decrease the marginal water use efficiency estimated from measured leaf transpiration and photosynthesis [58], but the consequences of this coupling on the theoretical optimal solutions have not been investigated yet.

It has also been argued that optimality in gas exchange cannot be sustained during midday (especially under limited soil water availability), because hydraulic constraints on water transport in the xylem become important, especially at low soil moisture [49,98]. When xylem cavitation limits water supply to the leaves, it effectively decouples the canopy from the soil water status, thus requiring additional constraints to the optimization. In particular, it would be interesting to assess the effects of coordination among plant hydraulic traits such as xylem and stomatal conductances (e.g., [15,61]) on the optimal water use.

3.3.3. Elevated atmospheric CO_2 concentration

As shown in Figs. 2 and 7, the proposed models fail in capturing the observed decline in stomatal conductance as atmospheric CO_2 concentration increases [75,76,99]. There are several possible explanations as to why a theory based only on water availability cannot capture such patterns. First, we neglected the down-regulation of photosynthetic capacity, which has been shown in grassland species [99], but not in *P. taeda* [39], where in fact the change in stomatal conductance between ambient and elevated CO_2 concentrations is small (Fig. 7(B)). If carboxylation capacity (k in our framework) declines with increasing c_a, the optimal g will also decline for a given value of the Lagrange multiplier (Table 2). However, when accounting for the dependence of λ on k, the net effects of down-regulation on the optimal trajectories become less clear. Future studies based on the derived optimal models will investigate these patterns.

It has been proposed that under elevated c_a plants will be more frequently light-limited, requiring to use nonlinear $A(c_i)$ curves, where A saturates at high c_a [73]. Our analyses highlighted different behaviors in the optimal solutions based on the linear (Eq. (35)) and nonlinear (Eq. (36)) photosynthesis models, as shown in Fig. 2. However, increasing the nonlinear character of the $A(c_i)$ curve, such as shifting from the C_3 to the C_4 grass, does not improve the predictive power of the models (Figs 2(B) and 7(B)). Hence, we surmise that other constraints may be important to capture plant responses to elevated atmospheric CO_2 concentrations.

Under elevated c_a, nitrogen may become a limiting factor, constraining photosynthetic capacity and altering allocation patterns [75,100]. Hence, accounting for nitrogen limitations in the optimization framework may be necessary [4,101]. Indeed, theoretical studies have shown that the marginal water use efficiency increases with c_a when also nitrogen dynamics are considered [78], and that plant responses to elevated c_a could be predicted using a coupled water–carbon–nitrogen optimization approach [13]. Moreover, at the leaf level, marginal water and nitrogen use efficiencies are anti-correlated under both ambient and elevated CO_2 concentrations [39]. Overall, these results suggest that including nitrogen availability constraints could improve the predictive power of the proposed theory.

4. Conclusions

Plants are hypothesized to maximize their C uptake and thus growth rate so as to utilize limited resources efficiently and achieve competitive advantages over other species. C uptake, however, is constrained by stomatal conductance, which also controls water losses to the atmosphere. Because water availability in the soil is limited, stomata are hypothesized to optimally regulate water losses to maximize C uptake, subject to the dynamic constraint imposed by soil moisture balance. Analytical solutions for this optimization problem are derived for different formulations, starting from the simplest case where soil moisture changes in time are neglected, to cases including uncontrolled water losses (due to physical processes or competition with other plants) and explicit consideration of water saving strategies (Table 2).

When soil moisture dynamics are neglected, the optimal stomatal conductance formulation derived in previous studies is recovered, where the Lagrange multiplier of the optimization (corresponding to the marginal water use efficiency, λ), remains an undetermined constant. While this formulation is useful to describe responses of stomata to rapid fluctuations in the environment (e.g., VPD) it cannot capture the responses to soil moisture changes or altered atmospheric CO_2 concentrations. Accounting for the dynamic constraint imposed by soil moisture over a dry-down overcomes these limitations and provide a time-varying, optimal stomatal conductance that declines as water availability decreases, and is sensitive to the water use strategy adopted by the plant. The marginal water use efficiency is shown to increase as soil moisture declines, but also to depend on the long-term CO_2 concentration, vapor pressure deficit, and mean duration of dry periods. In general, more xeric conditions (longer dry periods, higher VPD, and lower soil moisture) increase λ and decrease stomatal conductance, consistent with observations. However, plants grown under elevated atmospheric CO_2 are not predicted to decrease their stomatal conductance, contrary to observations.

While the proposed set of models allow comparing previous approaches under the same framework and explain some observed patterns, several questions remain open for future research. For example, the lack of sensitivity of stomatal conductance to elevated CO_2 concentrations suggests that the proposed water-based optimality approach may require additional constraints (e.g., nitrogen dynamics). Moreover, the feedback of stomatal conductance on leaf pressure and hence on photosynthetic capacity has been neglected, while it can have a major impact on the optimality conditions and predictions. Finally, we focused on an individual dry-down, therefore neglecting rainfall stochasticity, which introduces distributions of initial soil moisture values and dry-down durations, linking the previous hydrologic history to the current plant and soil water status. These remain open questions for future theoretical developments.

Acknowledgments

This work was supported by the US Department of Energy (DOE) through the Office of Biological and Environmental Research (BER) Terrestrial Carbon Processes (TCP) program (DE-SC0006967), by the Agriculture and Food Research Initiative from the USDA National Institute of Food and Agriculture (2011-67003-30222), by the US National Science Foundation (Frontiers in Earth System Dynamics – 1338694), by the Binational Agricultural Research and Development (BARD) Fund (IS-4374-11C), and by the project AgResource and an excellence grant from the Faculty of Natural Resources and Agricultural Sciences (Swedish University of Agricultural Sciences). We also thank Belinda E. Medlyn for stimulating discussions on different modeling approaches for plant gas exchange, Thomas P. Witelski for guidance on optimal control theory, and four anonymous reviewers whose comments improved the original manuscript.

Appendix A. Stomatal aperture *vs.* stomatal conductance as the control variable

This appendix shows that using stomatal conductance g instead of stomatal aperture u as the control variable does not alter the modeling results presented in the main text. The most common formulation to describe the maximum stomatal conductance (denoted by g_{max} and assumed constant at dry-down time scales) is given as [40,41,102],

$$g_{max} = \frac{B a_{max}}{l + c_e}, \tag{31}$$

where $B = d_m D_s/(a v_a)$, d_m is the molecular diffusivity of water vapor, and v_a is the molar volume of air, D_s is the stomatal density, a_{max} is the maximum area of the open stomatal pore, l is the stomatal pore depth, and $c_e = \sqrt{a_{max}\pi/4}$ accounts for interference among diffusion shells at the outside end of stomatal pores. Let the actual stomatal aperture (u) be given by $a_{max}u$, with $u = 1$ defining fully open stomata to achieve g_{max} and $u = 0$ defining stomata that are fully closed. Hence, g can now be explicitly linked to aperture u via

$$g(u) = \frac{B a_{max} u}{l + \frac{1}{2}\sqrt{\pi a_{max} u}}. \tag{32}$$

It is known that stomata regulate u via ion and sugar exchanges (partly controlled by ABA concentration) between guard cells and epidermal cells, which in turn cause the pressure differences driving stomatal opening [103–105]. It is this regulation of ion exchange that determines g at the leaf level. Now, the Hamiltonian in Eq. (4) must be revised so that u instead of g is the control variable. The necessary condition for optimal control can be written as a function of the control u (Eq. (4)) as $\partial H/\partial u = 0$. However, considering the dependence of conductance on aperture yields,

$$\frac{\partial H}{\partial u} = \frac{\partial H}{\partial g}\frac{\partial g}{\partial u} = 0, \tag{33}$$

where $\partial g/\partial u > 0$ for all u, because the function $g(u)$ in Eq. (32) is monotonically increasing. Accordingly, the optimization problem remains entirely controlled by the $\partial H/\partial g$ component with $\partial g/\partial u$ being divided out. Hence, all the g_{opt} formulations obtained are robust to the fact that the control variable was assumed to be g instead of u.

Appendix B. Relation between photosynthesis and stomatal conductance

An explicit link between photosynthesis and stomatal conductance can be obtained by coupling diffusion equations for water vapor and CO_2 supplied from the atmosphere through stomata to a model of the biochemical demand for carbon imposed by photosynthesis [31,32]. Employing a representation analogous to Eq. (9) and again assuming negligible aerodynamic resistance, CO_2 diffusion through stomata can be expressed as

$$A = g(c_a - c_i), \tag{34}$$

where c_a and c_i are the atmospheric and leaf internal CO_2 concentrations, respectively. To describe the biochemical demand for CO_2, a simplified approach that assumes a linear relation between leaf internal CO_2 concentration and biochemical demand is given as [56–58]

$$A = k c_i - r, \tag{35}$$

where k is the carboxylation efficiency and r indicates leaf respiration. The effect of light availability on photosynthesis can also be included through a dependence of k on incident radiation [56]. A more accurate description of light limitations could also be employed, where photosynthesis is limited by either CO_2 availability or light, or is co-limited by these two resources, leading to more complicated expressions [72,101,106]. While the proposed framework can accommodate any general biochemical demand function, in the current study we aim at obtaining analytical solutions using an approximated expression for photosynthesis. Supporting this line, it has been argued that Eq. (35) may be suitable in most conditions because plants tend to operate at the intersection between the Rubisco and RuBP regeneration limitation regimes [106]. Recent studies showed that, at least in some species, the effect of the nonlinearity in the $A(c_i)$ curve is relatively small over the range of internal CO_2 concentrations caused by changes in stomatal conductance during a drought, supporting this simplified relation [47,64].

The optimal solutions are different in light-limited conditions where the $A(c_i)$ curve is less sensitive to changes in internal CO_2 than in Eq. (35), as shown elsewhere [73,106]. The main steps in the derivations for a nonlinear $A(c_i)$ curve that would arise when accounting for light-limitation at elevated c_a are reported for completeness in Appendix C, and results for the linear and nonlinear cases are compared in Section 3. Metabolic limitations of photosynthesis caused by water stress could also be accounted for by expressing the carboxylation efficiency as a function of leaf water potential [95]. Because leaf water potential depends on the balance of water supplied to the leaf and evaporated through the stomata, explicitly including leaf water potential in Eq. (35) would introduce a further (albeit indirect) effect of g on A (see Section 3.3.2). As a starting point, this effect is neglected and k is regarded as an externally-imposed parameter dependent on light availability or temperature, but independent of the plant water status or soil moisture. We also neglect acclimation of k at elevated c_a (Section 3.3.3).

Appendix C. Nonlinear $A(c_i)$ curve

In this appendix the assumption of linear $A(c_i)$ curve (Eq (35)) is relaxed by adopting a more general nonlinear kinetic equation in the form (analogous to the equation developed for a single limitation by [107]),

$$A = \frac{a_1(c_i - c_p)}{a_2 + c_i} - r \approx \frac{a_1 c_i}{a_2 + c_i}, \tag{36}$$

where a_1 is the maximum photosynthetic rate, a_2 is the half-saturation constant, and c_p the compensation point. The values of the kinetic parameters depends on the predominant limitation to photosynthesis (RuBP regeneration or Rubisco) and might be computed for the case of co-limitation as well [106]. Employing the same optimization approach used for the linear model, and neglecting for simplicity compensation point and respiration, the optimal stomatal conductance is found as,

$$g_{opt}(t) = \frac{a_1}{(a_2 + c_a)^2}\left[\frac{a_2 + c_a - 2\alpha D\lambda(t)}{\sqrt{a_2 + c_a - \alpha D\lambda(t)}}\sqrt{\frac{a_2 c_a}{\alpha D\lambda(t)}} - a_2 + c_a\right]. \tag{37}$$

Because the nonlinearity in the photosynthesis equation does not affect the uncontrolled water losses, $\lambda(t)$ is obtained as before (Table 2). Eq. (37) recovers the result presented previously [64], where however $\lambda(t)$ was considered a fitting parameter.

In the case of constant uncontrolled losses ($c = 0$), $\lambda(t) = \lambda_0$, g_{opt} is constant, and the soil moisture trajectory remains linear (Eq. (20)). The relationship between λ_0 and the other parameters can be found by setting as before $x_{opt}(T) = 0$, obtaining,

$$\lambda_0 = \frac{a_1(a_2 - c_a) + (a_2 + c_a)\left[(a_2 + c_a)\sigma + \sqrt{a_1^2 + 2a_1(a_2 - c_a)\sigma + (a_2 + c_a)^2\sigma^2}\right]}{2\alpha D\sqrt{a_1^2 + 2a_1(a_2 - c_a)\sigma + (a_2 + c_a)^2\sigma^2}}, \tag{38}$$

where $\sigma = (x_0 - \beta T)/(\alpha DT)$.

When uncontrolled losses are assumed to be linear with soil moisture ($c = 1$), the Lagrange multiplier and the optimal stomatal conductance vary through time, resulting in the soil moisture trajectory (found by solving Eq. (16)),

$$x_{opt}(t) = \frac{a_1 e^{-\beta t}}{\beta(a_2 + c_a)^2}\left[(a_2 - c_a)(e^{\beta t} - 1)\alpha D + \frac{x_0\beta(a_2 + c_a)^2}{a_1} + 2\sqrt{\frac{a_2 c_a \alpha D}{\lambda_0}}\left(\sqrt{a_2 + c_a - \alpha D\lambda_0} - \sqrt{e^{\beta t}(a_2 + c_a - \alpha D\lambda_0 e^{\beta t})}\right)\right], \tag{39}$$

where the initial value of the Lagrange multiplier for the intensive water use strategy can be obtained numerically by setting $x_{opt} = 0$ at $t = T$. In contrast, for the conservative water use strategy the initial value of λ can be computed as $\lambda_0 = \Lambda e^{-\beta T}$, thus allowing to use Eq. (39) without further calculations.

The nonlinearities in the $A(c_i)$ curve are expected to predominantly impact the dependence of g_{opt} and λ on atmospheric CO_2 concentration [73,106]. To assess these effects, optimal solutions for the nonlinear photosynthesis model are compared to the approximated solutions based on linear photosynthesis in Figs. 2–4.

References

[1] Rosen R. Optimality principles in biology. Plenum Press; 1967.
[2] Eagleson PS. Ecohydrology. Darwinian expression of vegetation form and function. Cambridge University Press; 2002.
[3] Givnish TJ, editor. On the economy of plant form and function. Cambridge University Press; 1986. p. 736.
[4] Cowan I. Fit, fitter, fittest; Where does optimisation fit in? Silva Fennica 2002;36(3):745–54.
[5] Rodriguez-Iturbe I, Porporato A. Ecohydrology of water-controlled ecosystems. Soil moisture and plant dynamics Cambridge. Cambridge University Press; 2004.
[6] Caylor KK, Scanlon TM, Rodriguez-Iturbe I. Ecohydrological optimization of pattern and processes in water-limited ecosystems: a trade-off-based hypothesis. Water Resour Res 2009;45:W08407. http://dx.doi.org/10.1029/2008WR007230.
[7] Emanuel RE, D'Odorico P, Epstein HE. Evidence of optimal water use by vegetation across a range of North American ecosystems. Geophys Res Lett 2007;34(7).
[8] Franklin O, Johansson J, Dewar RC, Dieckmann U, McMurtrie RE, Brannstrom A, et al. Modeling carbon allocation in trees: a search for principles. Tree Physiol 2012;32(6):648–66.
[9] Guswa AJ. Effect of plant uptake strategy on the water-optimal root depth. Water Resour Res 2010;46:W09601. http://dx.doi.org/10.1029/2010WR009122.
[10] Hölttä T, Mencuccini M, Nikinmaa E. A carbon cost-gain model explains the observed patterns of xylem safety and efficiency. Plant Cell Environ 2011;34(11):1819–34.
[11] Magnani F, Mencuccini M, Grace J. Age-related decline in stand productivity: the role of structural acclimation under hydraulic constraints. Plant Cell Environ 2000;23(3):251–63.
[12] McCulloh KA, Sperry JS, Adler FR. Water transport in plants obeys Murray's law. Nature 2003;421(6926):939–42.
[13] McMurtrie RE, Norby RJ, Medlyn BE, Dewar RC, Pepper DA, Reich PB, et al. Why is plant-growth response to elevated CO_2 amplified when water is limiting, but reduced when nitrogen is limiting? A growth-optimisation hypothesis. Funct Plant Biol 2008;35(6):521–34.
[14] Schwinning S, Ehleringer JR. Water use trade-offs and optimal adaptations to pulse-driven arid ecosystems. J Ecol 2001;89(3):464–80.
[15] Manzoni S, Vico G, Katul G, Palmroth S, Porporato A. Optimal water-use strategies under unpredictable rainfall regimes. Water Resour Res [submitted for publication].
[16] Kirk DE. Optimal control theory. An introduction Englewood Cliffs, NJ. Prentice-Hall Inc.; 1970.
[17] Bejan A, Lorente S. The constructal law of design and evolution in nature. Philos Trans R Soc B Biol Sci 2010;365(1545):1335–47.

[18] Ozawa H, Ohmura A, Lorenz RD, Pujol T. The second law of thermodynamics and the global climate system: a review of the maximum entropy production principle. Rev. Geophys. 2003;41(4):1018. http://dx.doi.org/10.1029/2002RG000113.

[19] Kleidon A. A basic introduction to the thermodynamics of the Earth system far from equilibrium and maximum entropy production. Philos Trans R Soc B Biol Sci 2010;365(1545):1303–15.

[20] Martyushev LM, Seleznev VD. Maximum entropy production principle in physics, chemistry and biology. Phys Rep Rev Sec Phys Lett 2006;426(1):1–45.

[21] Dewar RC. Maximum entropy production and plant optimization theories. Philos Trans R Soc B Biol Sci 2010;365(1545):1429–35.

[22] Wang JF, Bras RL, Lerdau M, Salvucci GD. A maximum hypothesis of transpiration. J Geophys Res Biogeosci 2007;112(G3):G03010. http://dx.doi.org/10.1029/2006JG000255.

[23] Bejan A, Lorente S, Lee J. Unifying constructal theory of tree roots, canopies and forests. J Theor Biol 2008;254(3):529–40.

[24] Manzoni S, Vico G, Katul G, Palmroth S, Jackson RB, Porporato A. Hydraulic limits on maximum plant transpiration and the origin of the safety-efficiency tradeoff. New Phytol 2013;198(1):169–78.

[25] Niklas KJ, Enquist BJ. On the vegetative biomass partitioning of seed plant leaves, stems, and roots. Am Nat 2002;159(5):482–97.

[26] Iwasa Y, Roughgarden J. Shoot root balance of plants – optimal-growth of a system with many vegetative organs. Theor Populat Biol 1984;25(1):78–105.

[27] Buckley TN, Roberts DW. DESPOT, a process-based tree growth model that allocates carbon to maximize carbon gain. Tree Physiol 2006;26(2):129–44.

[28] Franklin O. Optimal nitrogen allocation controls tree responses to elevated CO_2. New Phytol 2007;174(4):811–22.

[29] Eagleson PS. Ecological optimality in water-limited natural soil-vegetation systems. 1: Theory and hypothesis. Water Resour Res 1982;18(2):325–40.

[30] Cowan I, Farquhar GD. Stomatal function in relation to leaf metabolism an environment. In: Integration of activity in the higher plants. Symposia of the society of experimental biology. Cambridge University Press; 1977.

[31] Cowan IR, Troughton JH. Relative role of stomata in transpiration and assimilation. Planta 1971;97(4):325–36.

[32] Farquhar GD, Sharkey TD. Stomatal conductance and photosynthesis. Annu Rev Plant Physiol Plant Mol Biol 1982;33:317–45.

[33] Vico G, Manzoni S, Palmroth S, Katul G. Effects of stomatal delays on the economics of leaf gas exchange under intermittent light regimes. New Phytol 2011;192(3):640–52.

[34] Cowan I. Stomatal behavior and environment. Adv Bot Res 1977;4:117–228.

[35] van den Honert TH. Water transport in plants as a catenary process. Discuss Faraday Soc 1948;3:146–53.

[36] Maurel C, Verdoucq L, Luu D-T, Santoni V. Plant aquaporins: membrane channels with multiple integrated functions. Annu Rev Plant Biol 2008;59(1):595–624.

[37] Johnson DM, McCulloh KA, Meinzer FC, Woodruff DR, Eissenstat DM. Hydraulic patterns and safety margins, from stem to stomata, in three eastern US tree species. Tree Physiol 2011;31(6):659–68.

[38] Sack L, Holbrook NM. Leaf hydraulics. Annu Rev Plant Biol 2006:361–81.

[39] Palmroth S, Katul G, Maier CA, Ward E, Manzoni S, Vico G, et al. On the complementary relationship between nitrogen and water use efficiencies among *Pinus taeda* L. leaves grown under ambient and enriched CO_2 environments. Ann Bot 2013;111(3):467–77.

[40] de Boer HJ, Lammertsma EI, Wagner-Cremer F, Dilcher DL, Wassen MJ, Dekker SC. Climate forcing due to optimization of maximal leaf conductance in subtropical vegetation under rising CO_2. Proc Natl Acad Sci USA 2011;108(10):4041–6.

[41] Franks PJ, Beerling DJ. Maximum leaf conductance driven by CO_2 effects on stomatal size and density over geologic time. Proc Natl Acad Sci USA 2009;106(25):10343–7.

[42] Maseda PH, Fernandez RJ. Stay wet or else: three ways in which plants can adjust hydraulically to their environment. J Exp Bot 2006;57(15):3963–77.

[43] Cowan I. Regulation of water use in relation to carbon gain in higher plants. In: Lange OE, Nobel PS, Osmond CB, Ziegler H, editors. Physiological plant ecology. II: Water relations and carbon assimilation. Springer-Verlag; 1982. p. 589–614.

[44] Cowan I. Economics of carbon fixation in higher plants. In: Givnish TJ, editor. On the economy of plant form and function. Cambridge: Cambridge University Press; 1986. p. 133–70.

[45] Farquhar GD, Schulze ED, Kuppers M. Responses to humidity by stomata of *Nicotiana glauca* L and *Corylus avellana* L are consistent with the optimization of carbon-dioxide uptake with respect to water-loss. Aust J Plant Physiol 1980;7(3):315–27.

[46] Lloyd J, Farquhar GD. C-13 discrimination during CO_2 assimilation by the terrestrial biosphere. Oecologia 1994;99(3–4):201–15.

[47] Katul G, Palmroth S, Oren R. Leaf stomatal responses to vapour pressure deficit under current and CO_2-enriched atmosphere explained by the economics of gas exchange. Plant Cell Environ 2009;32:968–79.

[48] Palmroth S, Berninger F, Nikinmaa E, Lloyd J, Pulkkinen P, Hari P. Structural adaptation rather than water conservation was observed in Scots pine over a range of wet to dry climates. Oecologia 1999;121(3):302–9.

[49] Konrad W, Roth-Nebelsick A, Grein M. Modelling of stomatal density response to atmospheric CO_2. J Theor Biol 2008;253(4):638–58.

[50] Manzoni S, Katul G, Fay PA, Polley HW, Porporato A. Modeling the vegetation-atmosphere carbon dioxide and water vapor interactions along a controlled CO_2 gradient. Ecol Model 2011;222(3):653–65.

[51] Schymanski SJ, Sivapalan M, Roderick ML, Hutley LB, Beringer J. An optimality-based model of the dynamic feedbacks between natural vegetation and the water balance. Water Resour Res 2009;45:W01412. http://dx.doi.org/10.1029/2008WR006841.

[52] Heroult A, Lin Y-S, Bourne A, Medlyn BE, Ellsworth DS. Optimal stomatal conductance in relation to photosynthesis in climatically contrasting Eucalyptus species under drought. Plant Cell Environ 2013;36(2):262–74.

[53] Zhou S, Duursma RA, Medlyn BE, Kelly JWG, Prentice IC. How should we model plant responses to drought? An analysis of stomatal and non-stomatal responses to water stress. Agr Forest Meteorol 2013;182–183:204–14.

[54] Lawlor DW, Tezara W. Causes of decreased photosynthetic rate and metabolic capacity in water-deficient leaf cells: a critical evaluation of mechanisms and integration of processes. Ann Bot 2009;103(4):561–79.

[55] Sethi SP, Thompson GL. Optimal control theory. Applications to management science and economics. Springer; 2005.

[56] Hari P, Mäkelä A, Korpilahti E, Holmberg M. Optimal control of gas exchange. Tree Physiol 1986;2:169–75.

[57] Lloyd J. Modeling stomatal responses to environment in *Macadamia integrifolia*. Aust J Plant Physiol 1991;18(6):649–60.

[58] Manzoni S, Vico G, Katul G, Fay PA, Polley W, Palmroth S, et al. Optimizing stomatal conductance for maximum carbon gain under water stress: a meta-analysis across plant functional types and climates. Funct Ecol 2011;25(3):456–67.

[59] Hari P, Mäkelä A. Annual pattern of photosynthesis in Scots pine in the boreal zone. Tree Physiol 2003;23(3):145–55.

[60] Porporato A, Daly E, Rodriguez-Iturbe I. Soil water balance and ecosystem response to climate change. Am Nat 2004;164(5):625–32.

[61] Manzoni S, Vico G, Katul G, Porporato A. Biological constraints on water transport in the soil-plant-atmosphere system. Adv Water Resour 2013;51:292–304.

[62] Daly E, Porporato A, Rodriguez-Iturbe I. Coupled dynamics of photosynthesis, transpiration, and soil water balance. Part I: Upscaling from hourly to daily level. J Hydrometeorol 2004;5(3):546–58.

[63] Fay PA, Kelley AM, Procter AC, Hui D, Jin VL, Jackson RB, et al. Primary productivity and water balance of grassland vegetation on three soils in a continuous CO_2 gradient: initial results from the lysimeter CO_2 gradient experiment. Ecosystems 2009;12(5):699–714.

[64] Katul G, Manzoni S, Palmroth S, Oren R. A stomatal optimization theory to describe the effects of atmospheric CO_2 on leaf photosynthesis and transpiration. Ann Bot 2010;105(3):431–42.

[65] Katul GG, Porporato A, Daly E, Oishi AC, Kim HS, Stoy PC, et al. On the spectrum of soil moisture from hourly to interannual scales. Water Resour Res 2007;43(5):W05428. http://dx.doi.org/10.1029/2006WR005356.

[66] Gollan T, Turner NC, Schulze ED. The responses of stomata and leaf gas-exchange to vapor-pressure deficits and soil-water content .3 in the sclerophyllous woody species *Nerium Oleander*. Oecologia 1985;65(3):356–62.

[67] Campbell GS, Norman JM. An introduction to environmental biophysics. 2nd ed. Springer; 1998.

[68] D'Odorico P, Ridolfi L, Porporato A, Rodriguez-Iturbe I. Preferential states of seasonal soil moisture: the impact of climate fluctuations. Water Resour Res 2000;36(8):2209–19.

[69] Berninger F, Hari P. Optimal regulation of gas-exchange – evidence from field data. Ann Bot 1993;71(2):135–40.

[70] Yang B, Pallardy SG, Meyers TP, Gu LH, Hanson PJ, Wullschleger S, et al. Environmental controls on water use efficiency during severe drought in an Ozark Forest in Missouri, USA. Global Change Biol 2010;16(8):2252–71.

[71] Hari P, Mäkelä A, Pohja T. Surprising implications of the optimality hypothesis of stomatal regulation gain support in a field test. Aust J Plant Physiol 2000;27(1):77–80.

[72] Arneth A, Lloyd J, Santruckova H, Bird M, Grigoryev S, Kalaschnikov YN, et al. Response of central Siberian Scots pine to soil water deficit and long-term trends in atmospheric CO_2 concentration. Global Biogeochem Cycles 2002;16(1):1005. http://dx.doi.org/10.1029/2000GB001374.

[73] Medlyn BE, Duursma RA, Eamus D, Ellsworth DS, Prentice IC, Barton CVM, et al. Reconciling the optimal and empirical approaches to modelling stomatal conductance. Global Change Biol 2011;17(6):2134–44.

[74] Monteith JL. A reinterpretation of stomatal responses to humidity. Plant Cell Environ 1995;18(4):357–64.

[75] Ainsworth EA, Rogers A. The response of photosynthesis and stomatal conductance to rising [CO_2]: mechanisms and environmental interactions. Plant Cell Environ 2007;30(3):258–70.

[76] Medlyn BE, Barton CVM, Broadmeadow MSJ, Ceulemans R, De Angelis P, Forstreuter M, et al. Stomatal conductance of forest species after long-term exposure to elevated CO_2 concentration: a synthesis. New Phytol 2001;149(2):247–64.

[77] Milly PCD. An analytic solution of the stochastic storage problem applicable to soil–water. Water Resour Res 1993;29(11):3755–8.

[78] Buckley TN. The role of stomatal acclimation in modelling tree adaptation to high CO_2. J Exp Bot. 2008;59(7):1951–61.

[79] Mäkelä A, Berninger F, Hari P. Optimal control of gas exchange during drought: theoretical analysis. Ann Bot 1996;77(5):461–7.

[80] Dekker SC, Vrugt JA, Elkington RJ. Significant variation in vegetation characteristics and dynamics from ecohydrological optimality of net carbon profit. Ecohydrology 2012;5(1):1–18.
[81] Launiainen S, Katul GG, Kolari P, Vesala T, Hari P. Empirical and optimal stomatal controls on leaf and ecosystem level $CO_{(2)}$ and $H_{(2)}O$ exchange rates. Agr Forest Meteorol 2011;151(12):1672–89.
[82] Turner NC, Schulze ED, Gollan T. The responses of stomata and leaf gas-exchange to vapor–pressure deficits and soil-water content .2 in the mesophytic herbaceous species *Helianthus-Annuus*. Oecologia 1985;65(3):348–55.
[83] Duursma RA, Kolari P, Peramaki M, Nikinmaa E, Hari P, Delzon S, et al. Predicting the decline in daily maximum transpiration rate of two pine stands during drought based on constant minimum leaf water potential and plant hydraulic conductance. Tree Physiol 2008;28(2):265–76.
[84] Zwieniecki MA, Holbrook NM. Confronting Maxwell's demon: biophysics of xylem embolism repair. Trends Plant Sci 2009;14(10):530–4.
[85] Fites JA, Teskey RO. CO_2 and water-vapor exchange of *Pinus taeda* in relation to stomatal behavior – test of an optimization hypothesis. Canadian Journal of Forest Research Revue Canadienne De Recherche Forestiere 1988;18(2):150–7.
[86] Grieu P, Guehl JM, Aussenac G. The effects of soil and atmospheric drought on photosynthesis and stomatal control of gas-exchange in three coniferous species. Physiol Plant 1988;73(1):97–104.
[87] Thomas DS, Eamus D, Bell D. Optimization theory of stomatal behaviour – II: Stomatal responses of several tree species of north Australia to changes in light, soil and atmospheric water content and temperature. J Exp Bot 1999;50(332):393–400.
[88] Duursma RA, Payton P, Bange MP, Broughton KJ, Smith RA, Medlyn BE, et al. Near-optimal response of instantaneous transpiration efficiency to vapour pressure deficit, temperature and $[CO_2]$ in cotton (*Gossypium hirsutum* L.). Agr Forest Meteorol 2013;168:168–76.
[89] Siqueira M, Katul G, Porporato A. Onset of water stress, hysteresis in plant conductance, and hydraulic lift: scaling soil water dynamics from millimeters to meters. Water Resour Res 2008;44(1):W01432. http://dx.doi.org/10.1029/2007WR006094.
[90] Tuzet A, Perrier A, Leuning R. A coupled model of stomatal conductance, photosynthesis and transpiration. Plant Cell Environ 2003;26(7):1097–116.
[91] van der Tol C, Meesters A, Dolman AJ, Waterloo MJ. Optimum vegetation characteristics, assimilation, and transpiration during a dry season. 1: Model description. Water Resour Res 2008;44(3):W03421. http://dx.doi.org/10.1029/2007WR006241.
[92] Kumagai T, Porporato A. Strategies of a Bornean tropical rainforest water use as a function of rainfall regime: isohydric or anisohydric? Plant Cell Environ 2012;35(1):61–71.
[93] Porporato A, Laio F, Ridolfi L, Rodriguez-Iturbe I. Plants in water-controlled ecosystems: active role in hydrologic processes and response to water stress – III. Vegetation water stress. Adv Water Resour 2001;24(7):725–44.
[94] Rodriguez-Iturbe I, D'Odorico P, Porporato A, Ridolfi L. Tree-grass coexistence in Savannas: the role of spatial dynamics and climate fluctuations. Geophys Res Lett 1999;26(2):247–50.
[95] Vico G, Porporato A. Modelling C_3 and C_4 photosynthesis under water-stressed conditions. Plant Soil 2008;313(1–2):187–203.
[96] Reichstein M, Tenhunen JD, Roupsard O, Ourcival JM, Rambal S, Miglietta F, et al. Severe drought effects on ecosystem CO_2 and H_2O fluxes at three Mediterranean evergreen sites: revision of current hypotheses? Global Change Biol 2002;8(10):999–1017.
[97] Williams M, Rastetter EB, Fernandes DN, Goulden ML, Wofsy SC, Shaver GR, et al. Modelling the soil-plant-atmosphere continuum in a *Quercus-Acer* stand at Harvard forest: The regulation of stomatal conductance by light, nitrogen and soil/plant hydraulic properties. Plant Cell Environ 1996;19(8):911–27.
[98] Buckley TN. The control of stomata by water balance. New Phytol 2005;168(2):275–91.
[99] Anderson LJ, Maherali H, Johnson HB, Polley HW, Jackson RB. Gas exchange and photosynthetic acclimation over subambient to elevated CO_2 in a C-3-C-4 grassland. Global Change Biol 2001;7(6):693–707.
[100] Dewar RC, Franklin O, Makela A, McMurtrie RE, Valentine HT. Optimal function explains forest responses to global change. Bioscience 2009;59(2):127–39.
[101] Buckley TN, Miller JM, Farquhar GD. The mathematics of linked optimisation for water and nitrogen use in a canopy. Silva Fennica 2002;36(3):639–69.
[102] Parlange JY, Waggoner PE. Stomatal dimensions and resistance to diffusion. Plant Physiol 1970;46(2):337.
[103] Assman SM, Zeiger E. Guard cell bioenergetics. In: Zeiger E, Farquhar GD, Cowan IR, editors. Stomatal function. Stanford, CA: Stanford University Press; 1987. p. 163–93.
[104] Buckley TN, Mott KA, Farquhar GD. A hydromechanical and biochemical model of stomatal conductance. Plant Cell Environ 2003;26(10):1767–85.
[105] Tardieu F, Davies WJ. Integration of hydraulic and chemical signaling in the control of stomatal conductance and water status of droughted plants. Plant Cell Environ 1993;16(4):341–9.
[106] Vico G, Manzoni S, Palmroth S, Weih M, Katul G. A perspective on optimal leaf stomatal conductance under CO_2 and light co-limitations. Agr Forest Meteorol 2013;182–183:191–9.
[107] Farquhar GD, Caemmerer SV, Berry JA. A biochemical-model of photosynthetic CO_2 assimilation in leaves of C-3 species. Planta 1980;149(1):78–90.